PHR1 and PHL1 mediate rapid high-light responses and acclimation to triose phosphate oversupply

Lukas Ackermann[1], Monika Müller[1], Alina Johanna Hieber[1], Maria Klecker[1*]

[1] Plant Physiology, University of Bayreuth, 95440 Bayreuth, Germany

[*]Address correspondence to: Maria Klecker, Department of Plant Physiology, University of Bayreuth, Universitätsstrasse 30, D-95447 Bayreuth, Germany. e-mail: maria.klecker@uni-bayreuth.de

Short title: PHR1 and PHL1 signal photosynthetic stress

ORCID IDs

Maria Klecker 0000-0001-5508-2363

Lukas Ackermann 0009-0009-8604-6029

ABSTRACT

Fluctuations in light intensity require immediate metabolic adjustment which includes reprogramming of both plastidial and nuclear gene expression, but the signaling pathways behind such responses are not fully understood. Here we report the identification of an early high-light responsive pathway in *Arabidopsis thaliana* that depends on PHOSPHATE STARVATION RESPONSE 1 (PHR1) and PHR1-LIKE 1 (PHL1) transcription factors involved in low phosphate (P_i) signaling. High-light treatment rapidly induced the accumulation of PHR1-responsive transcripts in wildtype plants grown under nutrient-sufficient conditions, but not in *phr1 phl1* double knockout plants. Differences in starch accumulation and ATP levels were detected between wildtype and *phr1 phl1* mutants subjected to high light, suggesting a link between P_i signaling, carbohydrate partitioning, and energy status during stress. In line with a function of PHR1/PHL1 upon triose phosphate accumulation, we observed that blocking starch biosynthesis in the *phr1 phl1* double mutant, by introducing the *agd1-1* allele, causes a severe growth defect. Phenotypes of the *adg1 phr1 phl1* triple mutant such as high-light sensitivity and growth restriction in the absence of exogenously supplied sucrose resemble the previously described double mutant *adg1 tpt-2*, lacking a functional copy of the TRIOSE PHOSPHATE/PHOSPHATE TRANSLOCATOR (TPT), and we show that P_i responses are disturbed in *adg1 tpt-2*. We propose that P_i sequestration by photosynthesis and import of P_i into the chloroplast transiently depletes cytosolic P_i reserves upon sudden increases in light intensity. The low-P_i sensing machinery in the nucleus consequently implements early high-light transcriptional responses, qualifying P_i as a new operational retrograde signal.

Introduction

Light as a source of energy with highly fluctuating availability needs to be efficiently captured by the photoautotrophic metabolism. This necessitates an enzymatic machinery capable of coping with rapid changes in metabolic flux, as well as the containment of overexcitation-induced hazards. Both challenges are met not only by post-transcriptional regulation of enzyme activity (reviewed in König et al. (2012), Matiolli et al. (2022)), but also by pronounced changes in mRNA abundance that occur within 30 minutes upon an increase in irradiance (Vogel et al., 2014; Suzuki et al., 2015; Huang et al., 2019). The latter mechanism depends on fast signal transmission between the chloroplast and the nuclear transcription machinery. Such communication is mediated by ‘primary’ retrograde signals (Dietz, 2015),

including redox cues and reactive oxygen species like H_2O_2 and singlet oxygen which are produced during photosynthetic reactions (Bechtold et al., 2008; Dietz et al., 2016). Additionally, increased electron transport activity and light-induced Calvin cycle activation promote the accumulation of primary products of carbon fixation (Dietz and Heber, 1984; Dietz and Heber, 1986) which may themselves act as signaling molecules (Häusler et al., 2014; Moore et al., 2014). Hence, induction of high-light specific gene expression partially depends on the triose phosphate/phosphate translocator (TPT) that mediates the exchange of triose phosphates or 3-phosphoglycerate (3-PGA) with inorganic phosphate (P_i) at the chloroplast envelope (Schneider et al., 2002; Vogel et al., 2014; Weise et al., 2019). A central function of the TPT in light acclimation and retrograde signaling was corroborated by the severe high-light dependent phenotypes of double mutants defective in the *TPT* and *ADG1* (for *ADP GLUCOSE PYROPHOSPHORYLASE 1*), encoding a small subunit of the ADP-glucose pyrophosphorylase complex (AGPase) which is required for the biosynthesis of transitory starch (Schmitz et al., 2012). Phenotypes of *adg1-1 tpt* double mutants include growth retardation, low diurnal changes in carbohydrate levels, and high chlorophyll fluorescence. These observations point towards an important role of photosynthate partitioning for retrograde signaling, however the identity of the primary sensors as well as signal transduction mechanisms are still unclear.

Phosphorus makes up about 2-30 permille of the plant dry mass (Kumar et al., 2019), as it is incorporated into a large subset of biomolecules. Systemic signaling of P_i availability and P_i distribution within the plant body mainly depend on a conserved gene family encoding PHOSPHATE STARVATION RESPONSE 1 (PHR1) and PHR1 LIKE (PHL) transcription factors of the MYB coiled-coiled type (Rubio et al., 2001; Zhou et al., 2008; Bustos et al., 2010; Thibaud et al., 2010; Sun et al., 2016). Simultaneous loss of *PHR1* and *PHL1* function affects the expression of at least 68 percent of the P_i starvation responsive genes in the shoots of Arabidopsis (*Arabidopsis thaliana)* (Bustos et al., 2010). A decrease in cellular P_i concentration impairs production of the inositol pyrophosphate species InsP8, relieving PHR1/PHLs of suppression by SPX (for SYG1/Pho81/XPR1) domain-containing proteins, thus linking transcription factor activity to P_i availability (Puga et al., 2014; Dong et al., 2019; Zhu et al., 2019; Ried et al., 2021). The transcriptional response to P_i scarcity leads to scavenging of external and internal P_i sources through phosphatase induction (Morcuende et al., 2007) and altered lipid metabolism (Misson et al., 2005; Pant et al., 2015b), anthocyanin biosynthesis (Nilsson et al., 2012; Liu et al., 2022; Li et al., 2023), and protection from photodamage (Nilsson et al., 2012), to name a selection. PHR1/PHLs are characterized as transcriptional activators (Nilsson et al., 2007; Bustos et al., 2010). Accordingly, direct targets of PHR1

(Bustos et al., 2010; Castrillo et al., 2017) are strongly upregulated upon P_i starvation and include genes such as *PHOSPHATE STARVATION-INDUCED GENE 2* (*PS2*; AT1G73010) (Hanchi et al., 2018), *MONOGALACTOSYLDIACYLGLYCEROL SYNTHASE 3* (*MGD3*; AT2G11810) (Kobayashi et al., 2004), and *GLYCEROPHOSPHODIESTER PHOSPHODIESTERASE 1/SENESCENCE-RELATED GENE 3* (*SRG3*; AT3G02040) (Cheng et al., 2011). Nevertheless, a subset of transcripts is specifically repressed under P_i-depleted conditions which can be accounted for by the induction of microRNAs (reviewed in Paz-Ares et al. (2022)), the induction of transcriptional repressors, as well as the modulation of genome accessibility (Barragán-Rosillo et al., 2021) through PHR1/PHLs activity.

P_i is unique among the macronutrients in that it is the only root-supplied element which is directly consumed by photosynthesis (Heldt and Rapley, 1970; Dietz and Heber, 1984). It has been shown experimentally that under high-CO_2 and high-light conditions, photosynthesis can indeed become limited by P_i supply to the chloroplast, both under P_i depleted and nutrient-rich conditions (Dietz and Foyer, 1986; Sivak and Walker, 1986). However, whether rapid increase in photosynthetic activity affects P_i homeostasis of the cell, is still unclear. In this study, we show that increments in light intensity trigger an early nuclear transcriptional response characteristic of P_i depletion which depends on *PHR1* and *PHL1*. Processes regulated by PHR1/PHL1 upon increased illumination contribute to photosynthetic acclimation since *phr1 phl1* mutants showed metabolic alterations compared to the wildtype when subjected to high-light stress. Moreover, analysis of the starch biosynthesis-deficient *adg1 phr1 phl1* triple mutant revealed an important function of P_i signaling when triose phosphate utilization is impaired. Aspects of the growth defects observed for *adg1 phr1 phl1* phenocopy the *adg1 tpt-2* mutant, suggesting that triose phosphate partitioning strongly affects P_i homeostasis. Together, we propose that PHR1/PHL1 mediate rapid photosynthetic acclimation upon sudden increases in light intensity by using P_i as a previously unknown operational retrograde signal.

Results

Acclimation to P_i starvation is disturbed in *adg1 tpt-2*

Photoassimilate allocation and utilization in the chloroplast and cytosol mainly determine the rate of P_i recycling from photosynthetic products. To address how the partitioning of phosphorylated assimilates affects P_i homeostasis, we examined the phenotypes of mutants defective in starch biosynthesis (*adg1-1*) and chloroplastic triose phosphate export (*tpt-2*) during P_i starvation in the presence of 14.61 mM (0.5 %) sucrose, and used anthocyanin production as a read-out for the induction of the P_i starvation response. In accordance with previous reports (Nilsson et al., 2007), wildtype seedlings accumulated anthocyanins when transferred to P_i-deficient conditions (Figure 1A, B). This was not observed for the *phr1-3 phl1* mutant. While *tpt-2* mutant seedlings were indistinguishable from the wildtype in terms of anthocyanin content, pigmentation was significantly enhanced upon P_i starvation in *adg1-1*. Surprisingly, this effect was fully reversed in the double mutant *adg1 tpt-2* which even accumulated much lower amounts of anthocyanins than the wildtype (Figure 1B). Nevertheless, root responses to P_i depletion such as root hair production were normal in *adg1 tpt-2* (Figure 1A). Hence, increased anthocyanin production of *adg1-1* upon P_i starvation almost fully relied on photoassimilate transport over the chloroplast envelope. To test whether increased anthocyanin accumulation in *adg1-1* also depends on the signaling pathway executed by PHR1/PHLs, we created a triple mutant by crossing *adg1-1* and *phr1-3 phl1*. The anthocyanin content did not increase in the *adg1 phr1 phl1* triple mutant in response to P_i starvation (Figure 1B), confirming a crucial function of PHR1/PHL1 signaling in this process even in the absence of ADG1 activity.

P_i deprivation is also known to induce starch accumulation in a *PHR1*-dependent manner (Figure 1C and Supplemental Figure 1), which likely involves AGPase activity (Nilsson et al., 2007). Furthermore, also soluble sugar contents rise in wildtype plants upon P_i limitation (Pant et al., 2015a). We reasoned that contrasting pigmentation behavior of the *adg1-1* and *adg1 tpt-2* seedlings under P_i-depleted conditions might be caused by differential sugar accumulation (Zirngibl et al., 2023). First, we analyzed starch contents of seedling shoots under P_i-sufficient and -deficient conditions. While shoots of *tpt-2* showed slightly higher levels of starch than wildtype, P_i depletion did not result in considerable starch production in *adg1-1* or any of the derived mutant lines (Figure 1C), confirming that the small AGPase subunit ADG1 is required for increased starch accumulation under P_i starvation. In agreement with impaired starch biosynthesis, hexose levels were increased in *adg1-1* shoots under P_i depletion compared to the

wildtype, and we observed a tendency towards higher sucrose levels in *adg1-1* (Figure 1C). None of these effects were seen in the *adg1 phr1 phl1* triple mutant, suggesting that sugar metabolism in *adg1-1* was under control of PHR1/PHL1 during P_i depletion (Figure 1C). Surprisingly, sugar levels were not correlated to anthocyanin production in either *tpt-2* or *adg1 tpt-2*: While P_i-depleted shoots of *tpt-2* contained higher glucose levels than wildtype, the contents of all three soluble sugar species analyzed were similar between shoots of *adg1 tpt-2* and the wildtype when grown on sucrose-supplemented media (Fig. 1C). Thus, anthocyanin production in response to P_i starvation was partially uncoupled from cellular sugar contents. Taken together, PHR1/PHL1 activity is required, but not sufficient for anthocyanin production under P_i starvation, which furthermore depends on adequate metabolite partitioning between chloroplasts and the cytosol. Furthermore, the phenotypes of the *adg1 tpt-2* double mutant indicate that P_i starvation responses are disturbed in this mutant.

P_i starvation gene expression is triggered by high light

The low-P_i phenotypes of *adg1-1* and *adg1 tpt-2* mutant lines indicated that P_i starvation responses are affected by photoassimilate distribution and utilization. This raised the question whether photoassimilate turnover also impacts on P_i homeostasis under non-starved conditions. More specifically, P_i signaling might be modulated by naturally occurring changes in triose phosphate metabolism, for example upon an increase in light intensity. To address this, we tested low-P_i marker gene expression upon sudden increments in photon flux density. Using quantitative RT-PCR (qRT-PCR), we first confirmed that in our experimental setup transcript levels of *SRG3*, *PS2*, *SPX1*, and *MGD3* were all strongly induced by P_i starvation, which mainly depended on *PHR1/PHL1* (Supplemental Figure 2A). Additionally, we analyzed transcript levels of a putative vacuolar P_i efflux transporter, *VPE1* (AT3G47420) (Ramaiah et al., 2011; Xu et al., 2019), and confirmed upregulation of this gene in the wildtype subjected to P_i starvation which was again strongly attenuated in *phr1-1 phl1* mutants (Supplemental Figure 2A). Furthermore, for the promoter sequences of *SPX1* (lacking the naturally occurring *Nco*I restriction site, *proSPX1*^{GC}), *MGD3*, and *SRG3*, we observed that PHR1 was able to induce the expression of *promoter::LUC* fusion constructs when transiently expressed in mesophyll protoplasts (Supplemental Figure 2B), confirming that *SPX1*, *MGD3*, and *SRG3* are targets of PHR1.

To examine responses to enhanced illumination, we grew wildtype and *phr1-1 phl1* mutant plants under nutrient-rich conditions on soil in an 8/16 hours (light/dark) photoregime.

After 5 weeks, photon flux density was increased to 320±30 µmol m^{-2} s^{-1} (high light) while the control group was kept under growth light conditions of 80±5 µmol m^{-2} s^{-1}. Using qRT-PCR, we detected a pronounced upregulation of *SRG3*, *SPX1*, and *VPE1* transcripts in wildtype plants already after 20 min of exposure to high light compared to control plants, as well as a slight increase in *MGD3* and *PS2* transcript abundance (Figure 2). In all five cases, the upregulation of gene expression was attenuated within 125 min in high light (Figure 2), indicating that response to P_i shortage constitutes an early consequence of increased irradiance. Notably, induction of P_i starvation marker transcripts was not observed in *phr1-1 phl1* mutant plants (Figure 2). *PHR1* expression itself was reported to depend on light (Liu et al., 2017). Importantly however, increasing the light intensity to 320±30 µmol m^{-2} s^{-1} did not affect *PHR1* transcript levels under our experimental conditions (Supplemental Figure 3), consistent with the accumulation of *PHR1* transcript being only responsive to changes in the very low fluence range (Liu et al., 2017).

GLUCOSE-6-PHOSPHATE/PHOSPHATE TRANSLOCATOR 2 (*GPT2*) is a light responsive gene (Athanasiou et al., 2010) which was also described to be induced by P_i starvation (Morcuende et al., 2007). Furthermore, high-light induced expression of *GPT2* was previously described to depend on *TPT* function (Kunz et al., 2010; Weise et al., 2019), and we noted that the promotor sequence of *GPT2* contains a PHR1 binding motif (GTATATTC) close to the transcriptional start site. Therefore, we tested if the *GPT2* promotor could be activated by PHR1 in a transient expression system using the *LUC* reporter gene. In fact, *PHR1* expression induced LUC reporter activity when protoplasts were co-transfected with the *proGPT2::LUC*$_{Firefly}$ construct (Supplemental Figure 2B). However, the responsiveness of *proGPT2* to *PHR1* expression was considerably lower than observed with the constructs harboring *proSPX1*^{GC}, *proSRG3* or *proMGD3* upstream of the reporter CDS. Consistent with weak PHR1-mediated induction of *proGPT2* in protoplast assays, and in contrast to the other tested P_i-starvation responsive genes, *GPT2* was upregulated by high light in both wildtype and *phr1-1 phl1* after 45 minutes, and transcript levels continued to rise upon stress during the course of the analysis (Figure 2). This indicated that PHR1/PHL1 are not involved in high-light mediated induction of *GPT2* expression. Moreover, we were not able to detect an effect of the *gpt2-1* allele (Niewiadomski et al., 2005) on carbohydrate accumulation under P_i depletion (Supplemental Figure 1), arguing against a major role of this gene for sugar homeostasis under P_i starvation. Thus, metabolite transport over the chloroplast membrane likely creates another signal which is responsible for *GPT2* induction under high light. While this pathway is not

affected by *phr1-1 phl1* mutation, the double mutant fails to induce other P_i-depletion responsive genes which are upregulated in the wildtype very early after a shift in light intensity.

Metabolic responses to increased light are impaired in *phr1 phl1* mutants

Given that transcription of P_i-starvation responsive genes was rapidly induced by high light, we asked if this response was of physiological significance during acclimation to increased radiation. To investigate this, we determined the changes in adenylates, sugar, and starch contents that occurred within 90 min upon an increase in photon flux density from 80±5 µmol m^{-2} s^{-1} to 320±30 µmol m^{-2} s^{-1} in rosette leaves of 5-weeks-old wildtype and *phr1-1 phl1* mutant plants. As shown in Figure 3A, increasing the light intensity caused a slight drop in ATP levels in leaves of *phr1-1 phl1* mutants, while no significant changes were seen in wildtype plants. Notably, the ratio of ATP/ADP was not affected by either the genotype or the high-light treatment (Figure 3A). In contrast, fructose, glucose, and sucrose levels increased in leaves of both wildtype and *phr1-1 phl1* mutants subjected to high light as compared to control light conditions (Figure 3B). Interestingly, total levels of glucose and fructose were slightly lower in *phr1-1 phl1* leaves subjected to high light compared to wildtype leaves (Figure 3B). However, the relative increments in sugar levels upon stress did not differ significantly between wildtype and *phr1-1 phl1* mutants (Figure 3C).

Unlike sugar levels, starch content under control conditions was higher in *phr1-1 phl1* mutants than in wildtype plants (Figure 3D). This may be related to the fact that *phr1-1 phl1* mutants manifest lower P_i levels in the shoots (Wang et al., 2018a) which allosterically activates AGPase (Figueroa et al., 2022). Exposure to higher light intensities further increased starch content in both wildtype and *phr1-1 phl1* (Figure 3D). However, while the starch content of wildtype leaves increased by 1.98-fold relative to control conditions, *phr1-1 phl1* mutant plants exhibited a significantly lower increase by only 1.62-fold (Figure 3D). Thus, sequestration of photoassimilates in transitory starch under high light conditions was affected by loss of *PHR1/PHL1* function.

Since both P_i starvation and high-light stress trigger anthocyanin production, we next analyzed the ability of *phr1 phl1* mutants to accumulate anthocyanins during high-light acclimation. As shown in Figure 3E, anthocyanin contents of *phr1 phl1* leaves after 3 days of high-light exposure were significantly lower than in wildtype leaves or in the single mutants *phr1-3* and *phl1*, while loss of *SPX1/2* function did not have any statistically significant effect. To exclude that *phr1 phl1* mutant plants were generally impaired in anthocyanin biosynthesis,

we subjected seedlings to chemically induced oxidative stress. Here, anthocyanin contents were not significantly different between wildtype, *phr1-3 phl1*, and *spx1 spx2* seedlings after 5 days of growth on paraquat-containing media (Supplemental Figure 4), indicating that anthocyanin biosynthesis was functional during reactive oxygen stress in *phr1-3 phl1* mutants.

Next, we asked whether metabolic abnormalities in the *phr1 phl1* mutants were related to differences in photosynthetic performance at the level of the thylakoid reactions. Therefore, we performed pulse-amplitude modulated (PAM) chlorophyll fluorometry on rosette leaves subjected to increased light. The efficiency of photosystem II photochemistry (ΦPSII) dropped to the same extent in both wildtype and *phr1-1 phl1* mutants upon exposure to increased illumination for 125 min (Figure 4A). After 125 min of treatment, also the maximum efficiency of PSII (F_v/F_m) had decreased significantly in the stressed plants of both genotypes (Figure 4B). As for ΦPSII, no difference was observed for F_v/F_m between wildtype and *phr1-1 phl1*. Thus, *PHR1/PHL1* function likely affected adenylate levels, starch metabolism and anthocyanin pigmentation of leaves under high-light stress in a manner independent of the thylakoid reactions.

PHR1/PHL1 function is important when triose phosphate utilization is limited

Our observations indicated that P_i-starvation signaling might be important during a shift to higher light intensities. We hypothesized that this might be related to transient imbalances of triose phosphate production and P_i recycling that occur upon changes in photosynthetic activity. In order to address this, we tried to genetically mimic the otherwise transient state of insufficient P_i recycling from photosynthetic products. In the *adg1-1* mutant, disruption of starch biosynthesis leads to continuous limitation in triose phosphate utilization. Hence, we examined the phenotypes of the *adg1 phr1 phl1* triple mutant to assess the importance of PHR1/PHL1 signaling during triose phosphate overaccumulation.

Strikingly, when grown under conditions with a short photoperiod (8 hours), *adg1 phr1 phl1* mutant plants exhibited a strong growth defect that was apparent in a reduction in both leaf size and leaf number compared to *adg1-1* single and *phr1-3 phl1* double mutants (Figure 5A, B). Under long-day conditions (16 hours photoperiod), the reduction in rosette size was less pronounced, but *adg1 phr1 phl1* mutant plants exhibited premature leaf senescence with symptoms already visible at the age of 25 days (Figure 5A, arrow). Accelerated leaf senescence is also seen in *phr1 phl1* double mutants particularly under P_i deprived conditions (Bustos et al., 2010) (Figure 1A), but initiates later at the age of approximately 35 days when

grown under standard conditions on soil (Figure 5B) (Wang et al., 2018a). Furthermore, transition to flowering was much delayed in *adg1 phr1 phl1* compared to the parental lines (Figure 5C). Notably, delayed onset of the regenerative phase is a phenotype already inherent to both the *adg1-1* (Matsoukas et al., 2013) and *phr1 phl1* (Supplemental Figure 5) mutants.

We noted that the photoperiod-dependent reduction in rosette size seen for *adg1 phr1 phl1* was reminiscent of the phenotype of the *adg1 tpt-2* mutant (Figure 5A). Thus, we tested the ability of *adg1 phr1 phl1* to adapt to higher light intensities, since high-light sensitivity was also reported for the *adg1 tpt-2* mutant (Schmitz et al., 2012). In fact, seedling shoot growth of *adg1 phr1 phl1* and *adg1 tpt-2* was reduced to a similar extent when grown under high-light conditions (Figure 5D and Supplemental Figure 6). Moreover, growth of *adg1 phr1 phl1* mutants under high light was promoted by exogenously supplied sucrose (Figure 5D), as it was described for *adg1 tpt-2* (Heinrichs et al., 2012; Schmitz et al., 2012). When seedlings were grown on vertically positioned petri dishes, it became evident that sucrose strongly stimulated root growth of both *adg1 phr1 phl1* and *adg1 tpt-2* particularly under high-light conditions (Supplemental Figure 7). Interestingly, when analyzing vertically grown seedlings, we observed a tendency for high-light sensitivity of shoot growth also for the *adg1-1* single and *phr1-3 phl1* double mutant lines (Supplemental Figure 6A). Likewise, this effect could be alleviated by exogenously supplied sucrose. Notably, high-light sensitivity of *phr1-3 phl1* was more pronounced under high-P_i (2.5 mM) than low-P_i (0.25 mM) growth conditions (Supplemental Figure 6A), supporting the hypothesis that PHR1/PHL1 play a role for high-light adaptation also under P_i sufficiency. It was concluded from these experiments that lack of *PHR1/PHL1* compromises plant growth under conditions of high triose phosphate accumulation such as high light or when starch biosynthesis is genetically blocked.

Carbohydrate signaling is affected during P_i deprivation

Seedling growth of *phr1-3 phl1* (Supplemental Figure 6A) and *adg1 phr1 phl1* (Figure 5D and Supplemental Figure 7) was supported by sucrose supplementation particularly under high light, and high-light induced starch accumulation was reduced in *phr1-1 phl1* mutants (Figure 3D). Both observations suggest that *phr1 phl1* mutation leads to alterations in carbohydrate metabolism. To address the question of how carbohydrate signaling might be modulated under conditions when PHR1 activity is high, we re-analyzed published transcriptome data obtained from seedlings subjected to P_i depletion (Bustos et al., 2010), and from rosette plants exposed to a low CO_2 environment (Bläsing et al., 2005). Among the

transcripts which were most strongly upregulated in shoots of *phr1-1 phl1* under P_i depletion relative to the wildtype, the majority was repressed by P_i depletion in the wildtype (Supplemental Figure 8). This supports a function of PHR1/PHL1 in the downregulation of certain transcripts under P_i depletion, as previously suggested (Bustos et al., 2010). Interestingly, we noted that many of these transcripts were also responsive to carbon starvation (Bläsing et al., 2005) (Supplemental Figure 8).

We chose four of the transcripts which were upregulated in *phr1-1 phl1* compared to the wildtype under P_i starvation for further analysis: The circadian regulators *BASIC LEUCINE ZIPPER 63* (*bZIP63*) (Baena-González et al., 2007; Frank et al., 2018) and *REVEILLE 1* (*RVE1*) (Rawat et al., 2009), as well as *BETA-XYLOSIDASE1* (*BXL1*), and *SENESCENCE1/DARK INDUCIBLE1* (*SEN1*/*DIN1*), a putative target gene of bZIP63 (Matiolli et al., 2011). In qRT-PCR analysis of seedlings grown on sucrose-containing media with or without P_i, both *bZIP63* and *BXL1* were down-regulated in shoots of wildtype seedlings exposed to P_i depletion, whereas no significant changes were detected for *phr1-1 phl1* mutants (Figure 5E), potentially reflecting sugar accumulation in the wildtype (Supplemental Figure 1). In contrast, transcript levels of *SEN1* and *RVE1* were highly increased in *phr1-1 phl1* mutants under P_i deprivation, but no significant changes were seen in the wildtype background (Figure 5F). Thus, expression of carbohydrate responsive genes, including circadian-clock associated genes, differs between wildtype and *phr1-1 phl1* mutants under P_i depletion.

Transcription in the *adg1 tpt-2* mutant exhibits a constitutive P_i-starvation signature

The phenotypic similarities of the *adg1 phr1 phl1* and *adg1 tpt-2* mutants suggested that triose phosphate partitioning and P_i signaling share some physiological consequences, supporting that triose phosphate utilization affects cellular P_i homeostasis. To assess if PHR1/PHLs activity was altered in *adg1 tpt-2*, we analyzed P_i-starvation marker gene expression in rosette leaves of plants grown for 5 weeks under an 8-hours light regime and a moderate light intensity of 90±10 µmol m^{-2} s^{-1}. Surprisingly, *SRG3*, *PS2*, *SPX1*, *VPE1* and *MGD3* were all significantly upregulated in shoots of soil-grown *adg1 tpt-2* plants compared to wildtype or the single *adg1-1* and *tpt-2* mutants (Figure 6A), indicating high activity of PHR1 in shoots of *adg1 tpt-2*. Moreover, *bZIP63* expression was significantly reduced in both *adg1-1* and *adg1 tpt-2*, whereas we observed a slight increase in *bZIP63* transcript levels in rosette leaves of *tpt-2* mutants (Figure 6A). To test if altered expression of P_i-starvation associated genes in *adg1 tpt-2* was linked to reduced P_i levels in the shoots of the mutant, we next

determined P_i contents in 5-weeks-old rosette leaves grown on soil under moderate light. Interestingly, the P_i content was not reduced in shoots of *adg1 tpt-2* compared to the wildtype, but P_i levels were even found to be higher than in *adg1-1* single mutants (Figure 6B). Thus, P_i loading of the shoots was not impaired in *adg1 tpt-2*, and P_i-starvation responsive genes were instead constitutively upregulated in *adg1 tpt-2* rosette leaves, indicating high PHR1 activity even under nutrient-sufficient physiological conditions in this mutant.

Discussion

The observations presented herein establish that the P_i response machinery involving the transcription factors PHR1 and PHL1 is capable of sensing early high-light stress, and we provide evidence that *PHR1/PHL1* contribute to the rapid adjustment of carbohydrate metabolism during changes in light intensity. P_i consumption by photosynthesis is thus hypothesized to generate a chloroplast-to-nucleus retrograde signal. In fact, P_i qualifies as a subcellular signal by a number of criteria: 1) [P_i] changes immediately and gradually in response to photoassimilation (Stitt et al., 1980; Dietz and Heber, 1984; Robinson and Giersch, 1987); 2) multiple transport proteins at the organellar membranes (Fabiańska et al., 2019) ensure rapid transmission of the [P_i] signal; 3) signal propagation is based on diffusion and does not rely on acceptor and donor molecules; 4) P_i exhibits low toxicity within a wide concentration range; 5) a highly responsive signaling machinery is present in the cytosol and nucleus.

Increase in light intensity creates a transient low-P_i signal

Under conditions where carboxylation exceeds subsequent metabolic capacities of the chloroplast, such as high light (Laisk et al., 1991), low temperature (Stitt and Grosse, 1988), and low oxygen (Klecker et al., 2014), large pools of 3-phosphoglycerate may build up which can enter the cytosol via the TPT (Schneider et al., 2002). By the nature of the transport mechanism, this depletes the cytosol of P_i, and it is assumed that P_i import from the vacuole is too slow to balance against very short-term changes in P_i demand (Woodrow et al., 1984). In accordance with these considerations, we found that transcription exhibits a P_i-starvation signature in Arabidopsis rosette leaves subjected to light increase already after 20 min of stress (Figure 2). This response depended on *PHR1/PHL1* function, indicating that light stress activated the cytosolic and nuclear P_i sensing machinery (Figure 7). PHR1 target genes which showed enhanced expression in our experimental setup included *SRG3*, *SPX1*, and *VPE1*, and

all three transcripts also showed early enrichment upon high-light treatment within a time-resolved transcriptome analysis previously described by Huang et al. (2019). Both *SRG3* and *VPE1* expression might be suitable to rapidly increase P_i availability in the cytosol via glycerophosphodiester turnover (Cheng et al., 2011) and vacuolar P_i efflux (Xu et al., 2019), respectively. In contrast, *SPX1* upregulation potentially contributes to the rapid tempering of the transcriptional response which was quenched already after 2 hours of treatment (Figure 2). Next to negative feed-back by SPX1, adjustment of triose phosphate turnover by post-translational activation of sucrose (Stitt et al., 1983; Preiss, 1984) and starch (Preiss, 1988; Hendriks et al., 2003) biosynthesis would be expected to attenuate any condition of light-induced P_i depletion within relatively short time. Therefore, long-term P_i-starvation responses such as lipid remodeling are rather unlikely to occur upon light intensity increases as long as higher P_i demand can be sufficiently covered by uptake via the roots or release of P_i storage within the mesophyll cell. Consistent with this assumption, induction of *MGD3* transcript was moderate in our experimental setup (Figure 2). Interestingly however, van Rooijen et al. (2018) observed upregulation of PHR1 target genes with involvement in lipid remodeling after 1 hour of irradiance increase. Thus, it will be exciting to learn from future experiments whether P_i signaling also contributes to the changes that can be seen in the lipid composition of leaves under different light conditions (Yu et al., 2021).

P_i sensing impacts on carbohydrate and energy metabolism upon light increase

The induction of genes related to P_i mobilization upon high light might be considered a transcriptional feedback response initiated in order to sustain substrate supply for metabolic reactions. Classification of P_i as a retrograde signal requires, beyond that, P_i signaling to affect further physiological processes by calibrating nuclear gene expression according to the status of the plastids. Crucially, this study shows that mutants defective in *PHR1* and *PHL1* which fail to mount a transcriptional response related to P_i starvation, develop metabolic abnormalities in the leaves within only 1.5 hours of high-light treatment (Figure 3A-D), and exhibit lower levels of anthocyanin pigmentation after 3 days of treatment (Figure 3E). ATP levels measured after 1.5 hours of high-light exposure were significantly lower in leaves of *phr1-1 phl1* mutant plants compared to wildtype plants (Figure 3A), whereas ΦPSII values were indistinguishable (Figure 4A). Given that ΦPSII can be interpreted as a measure of the linear electron transport rate (Maxwell and Johnson, 2000), this indicates that ATP synthesis at the thylakoids was likely not affected by loss of *PHR1/PHL1* function. This is consistent with the assumption that P_i

sequestration upon photosynthetic activity does not compromise stromal P_i levels and thus ATP synthesis as long as phosphorylated metabolites are exchanged with the cytosol via P_i antiport systems (Robinson and Giersch, 1987). In contrast, it would be conceivable that the P_i concentration outside of the chloroplast might drop below levels required for efficient mitochondrial ATP synthesis in the *phr1-1 phl1* mutant. In fact, a decline in ATP levels can also be observed in plants under P_i-deficient growth conditions (Zhu et al., 2019; Riemer et al., 2021), but the reason for this is currently unknown.

While starch levels under standard light conditions were slightly higher in *phr1-1 phl1* rosettes compared to wildtype, the high-light induced relative increase in starch content was considerably higher in wildtype leaves compared to the mutant (Figure 3D). This delay in the activation of starch biosynthesis is remarkable, given that post-translational activation of AGPase by the 3-PGA/P_i ratio is probably high in *phr1-1 phl1* leaves which manifest chronically low P_i contents (Wang et al., 2018a). Similar to what can be seen under P_i deprivation (Supplemental Figure 1) (Nilsson et al., 2007), the difference in starch accumulation observed between wildtype and *phr1-1 phl1* mutants upon transfer to high light was not reflected by changes in soluble sugar contents (Figure 3B, C). Together with our finding that photosynthetic capacity is wildtype-like in *phr1-1 phl1* mutants subjected to high-light stress (Figure 4), this suggests that starch production is rather not limited by photosynthetic precursor production in *phr1-1 phl1*. Hence, it is likely that PHR1/PHL1 directly regulate photoassimilate partitioning towards starch biosynthesis. Expression of *APL3* (AT4G39210) encoding a large subunit of AGPase, or *GGBS1* (AT1G32900), coding for a granule-bound starch synthase have been described to be induced by P_i starvation (Morcuende et al., 2007; Bustos et al., 2010; Wang et al., 2018b), and might contribute to both P_i-starvation and high-light induced starch accumulation.

P_i signaling is crucial under conditions of triose-phosphate oversupply

Prevention of starch production during P_i restriction leads to higher sugar and anthocyanin levels in the shoots (Figure 1). The observation is consistent with sugars being formed upon recycling of phosphorylated metabolites (Morcuende et al., 2007), and starch serving as a carbon sink in P_i-deprived plants (Hammond and White, 2008; MacNeill et al., 2017). Neither sugar accumulation, nor transitory starch or anthocyanin production take place in *phr1 phl1* mutant seedlings subjected to P_i depletion (Figure 1 and Supplemental Figure 1). Nevertheless, prohibition of starch biosynthesis by introduction of the *adg1-1* allele into this

mutant background produced a pronounced growth defect already visible at the seedling stage (Figure 5A, B, D and Supplementary Figures 6, 7). Growth of the *adg1 phr1 phl1* triple mutant was further impaired by higher light intensities (Figure 5D and Supplemental Figure 6), a condition that reinforces triose phosphate generation. These observations lead to the conclusion that *PHR1/PHL1* function is crucial in the *adg1-1* knockout situation, demonstrating the necessity for low-P_i signaling when photoassimilate consumption is constrained. Next to growth retardation, the *adg1 phr1 phl1* mutant showed a delay in the onset of flowering (Figure 5C), and benefited from exogenous sucrose supply in terms of both shoot and root growth (Figure 5D and Supplemental Figures 6, 7). Both late flowering (Wahl et al., 2013) and inhibition of primary root growth (Smith and Stitt, 2007) indicate that *adg1 phr1 phl1* plants suffer from carbohydrate starvation in the absence of external sucrose supply.

Interestingly, transcriptional changes observed on wildtype and *phr1-1 phl1* mutant plants under P_i deprivation also indicate that PHR1/PHL1 maintain sugar homeostasis when P_i availability is low (Figure 5E, F and Supplemental Figure 8). In agreement, strong increments in the levels of amino acids and oligosaccharides such as raffinose and kestose were reported for wildtype but not *phr1* mutants under P_i depletion (Pant et al., 2015a). Notably, oligosaccharide production facilitated by PHR1/PHL1 might serve as an alternative carbohydrate sink in the *adg1-1* mutant, and could support carbon supply of the starchless mutant during the night. This would be consistent with the observation that *adg1 phr1 phl1* was more strongly constrained by diel cycles with short light phases (Figure 5A). Similarly, oligosaccharide and amino acid accumulation triggered by the low-P_i signaling module could support carbohydrate homeostasis during high-light stress by maintaining P_i/C(/N) balance, and might even be suitable to prepare for potential osmotic stress as a likely consequence of high light in a natural environment. In line with this, a function of PHR1/PHL1 in proline accumulation and drought resistance has been reported (Aleksza et al., 2017; Scheible et al., 2023). It is difficult to dissect direct effects of P_i signaling from secondary consequences of P_i-deprived metabolism. Thus, metabolic differences of *adg1 phr1 phl1* mutants grown under short and long photoperiods might reveal new insights into how carbon fluxes are modulated by P_i signaling.

P_i signaling is affected in *adg1 tpt-2*

Strikingly, growth defects and high-light sensitivity of *adg1 phr1 phl1* are paralleled by the phenotypes of the *adg1 tpt-2* mutant (Figure 5A, D and Supplemental Figures 6, 7),

indicating that photoassimilate allocation and P_i signaling to some extent overlap in terms of their physiological consequences. Even under P_i sufficient growth conditions, we found that *adg1 tpt-2* exhibits a signature of P_i-starvation responsive gene expression (Figure 6), raising the question how insufficient export of photosynthetic products could generate a situation of high PHR1 activity. In the *adg1 tpt-2* mutant, a pronounced fraction of cytosolic/chloroplastic P_i can be assumed as metabolically unavailable, given that starch biosynthesis is prevented by *adg1-1* mutation, while sucrose production during the course of the day remains at much lower levels compared to *adg1-1* (Schmitz et al., 2012) (Figure 7). Hence, bulk release of P_i in *adg1 tpt-2* might be restricted to glycolysis and vacuolar phosphatase activity acting on phosphorylated intermediates such as phosphoenolpyruvate (Ohnishi et al., 2018). This would cause unequal intracellular pool sizes of free P_i, facilitating PHR1 activity in the cytosol/nucleus, while vacuolar P_i stores are high (Figure 6).

In fact, imbalances of intracellular P_i pools would affect both *PHR1*-dependent and independent (Osorio et al., 2019; Nam et al., 2021) P_i-responsive pathways. Such inadequate signaling could even contribute to the pleiotropic defects observed for *adg1 tpt-2* mutants (Schmitz et al., 2012), for example by altering lipid composition, or by the regulation of photosynthesis-associated genes (Morcuende et al., 2007; Bustos et al., 2010; Barragán-Rosillo et al., 2021; Nam et al., 2021). Interestingly, we also found that transcript levels of the circadian regulator bZIP63 were downregulated both by P_i depletion (Figure 5E), and in the *adg1 tpt-2* mutant (Figure 6). Given that *adg1 tpt-2* is characterized by overall low carbohydrate levels (Schmitz et al., 2012), *bZIP63* expression appears to be uncoupled from sugar levels in this mutant situation. Our observations open up the possibility that P_i signaling could be involved in this regulation which will be an exciting topic to address in the future.

Conclusions

High-light stress requires immediate responses to avert damage to cellular components. As a potential mode of sensing excess photosynthetic activity, we describe a function of the P_i-sensing machinery involving PHR1 and PHL1 transcription factors under nutrient replete growth conditions. We propose that P_i sequestration into phosphorylated photoassimilates and metabolite exchange across the chloroplast membrane causes transient P_i restriction in the cytosol and nucleus. This activates PHR1/PHL1 proteins to mobilize cellular P_i and to support acclimation responses such as starch biosynthesis. The finding that P_i signaling is disturbed in

the *adg1 tpt-2* mutant emphasizes that PHR1/PHL activity constitutes a so-far underestimated contributor to retrograde signaling of photosynthetic status.

Materials and Methods

Plant material

All Arabidopsis plants used in this study are in the background of the Columbia-0 accession. The *phr1-3* (AT4G28610; SALK_067629C) (Nilsson et al., 2007) and *phl1* (AT5G29000; SAIL_731_B09) (Klecker et al., 2014) lines were described previously and the derived homozygous double mutant *phr1-3 phl1* was a kind gift of Angelika Mustroph (University of Bayreuth). The double mutant *phr1-1 phl1* (Bustos et al., 2010) was backcrossed to *phl1* in order to remove a transgene containing the *NPTII* cassette which was previously introduced for isolation of the *phr1-1* allele (Rubio et al., 2001). All experiments were performed with the homozygous double mutant *phr1-1 phl1* lacking the *NPTII* cassette. The double mutant *spx1 spx2* was described earlier (Puga et al., 2014). Knockout lines *adg1-1* (At5g48300) (Lin et al., 1988), *tpt-2* (At5g46110; SALK_073707.54.25.x) and *adg1 tpt-2* (Schmitz et al., 2012) were kindly provided by Rainer E. Häusler (University of Cologne). *gpt2-1* (AT1G61800; GK-454H06) was obtained from The Nottingham Arabidopsis Stock Centre (NASC) and was described previously (Niewiadomski et al., 2005). Primer sequences used for genotyping are listed in Table S1. Homozygous insertion mutants were verified using the following primer combinations: *PHR1* WT: PHR1_F/PHR1_R; *phr1-3* T-DNA: LBb1/PHR1_R; *PHL1* WT: PHL1_F/PHL1_R; *phl1* T-DNA: PHL1_F/LB3; *TPT* WT: TPT_F/TPT_R; *tpt-2* T-DNA: *tpt-2*_F/LBb1; *GPT2* WT: GPT2_F/GPT2_R; *gpt2-1* T-DNA: GK-LB/GPT2_R. To generate the *adg1 phr1 phl1* triple mutant, *adg1-1* was crossed to *phr1-3 phl1*. Homozygous *adg1-1* mutants were identified by screening for starch-free phenotypes by iodine staining at the end of the photoperiod. Homozygosity of the *phr1-1* allele was verified by Sanger sequencing (Macrogen Europe, Amsterdam) of the PCR product of PHR1_F/PHR1_R using primer PHR1_R.

Cultivation conditions

Seeds were stratified for 64 hours at 4°C in the dark. For vegetative growth, plants were germinated and grown in an 8 h/16 h (light/dark) cycle on soil consisting of seeding compost, universal soil, and vermiculite mixed in a 3:3:1 ratio. For high-light experiments, the plants

were additionally fertilized once directly after pricking at the age of 10 days using a complete mineral mixture (Wuxal Super, Aglukon Spezialduenger, Duesseldorf, Germany) according to the manufacturer's instructions. For seedling experiments, seeds were surface sterilized by chlorine gas exposure and transferred to solidified Arabidopsis growth media as described in the figure legends. Seedlings were grown under 16 h/8 h light/dark cycles. For paraquat treatments, seedlings were germinated on agar-solidified media containing full-strength Murashige and Skoog (MS) salts and grown for 10 days before transfer to MS media with or without 1 µM paraquat dichloride hydrate (#36541, Riedel-de Haën, Hannover, Germany). If not indicated otherwise, growth light was set to 90±10 µmol m^{-2} sec^{-1} and monitored using an illuminance meter.

P_i-starvation experiments

For P_i-starvation experiments, seeds were germinated on medium containing MS salts at full strength together with 0.8 % (w/v) phytoagar (Duchefa Biochemie, Haarlem, The Netherlands) and 0.5 % (w/v) sucrose. After 5-10 days of growth (see figure legends), seedlings were transferred to P_i media (0.5 % (w/v) sucrose; 20 mM 2-(N-Morpholino)-ethane sulphonic acid; 2.5 mM KNO_3; 1 mM $MgSO_4$; 1 mM $Ca(NO_3)_2$; 2.5 mM KH_2PO_4; 25 µM Fe-EDTA; 35 µM H_3BO_3; 7 µM $MnCl_2$; 0.25 µM $CuSO_4$; 0.5 µM $ZNSO_4$; 0.1 µM $NaMoO_4$; 5 µM NaCl; 0.005 µM $CoCl_2$; pH 6) solidified by 0.8 % (w/v) agar (adopted from Härtel et al. (2000)). For P_i depleting conditions, KH_2PO_4 was omitted, and Fe-EDTA was reduced to 10 µM in order to minimize low-P_i induced iron toxicity (Ward et al., 2008). Seedling shoots were harvested after 7-8 days of growth on P_i differing media (see figure legends). For horizontally grown seedlings, MS salts were used at ½ concentrations and 0.6 % (w/v) agar were applied. For the experiment shown in Figures S6 and S7, P_i medium was used containing either 0.25 mM KH_2PO_4/10 µM Fe-EDTA, 2.5 mM KH_2PO_4/25 µM Fe-EDTA, or 2.5 mM KH_2PO_4/25 µM Fe-EDTA +50 mM sucrose.

Vector construction

Standard molecular cloning procedures were applied. Primer sequences used for cloning are listed in table S1. The firefly *LUCIFERASE* reporter plasmid *pBT10-proMGD3::LUC*$_{Firefly}$ and the *pHBTL-p35S::3HA-GFP* effector plasmid (Klecker et al., 2014), as well as the *pBT10-p35S::LUC*$_{Renilla}$ normalization plasmid (Bäumler et al., 2019) have been described elsewhere.

For details on cloning *proSPX1*^{GC}, *proSRG3*, *proMGD3*, *proGPT2,* and the *PHR1* effector construct, refer to the supplemental methods.

Anthocyanin determination

Anthocyanin contents were determined with few changes as described in (Vandenbussche et al., 2007). In brief, 40-70 mg of seedling shoots or rosette leaf material were frozen in liquid nitrogen and ground in a bead mill (MM400, Retsch, Haan, Germany). The frozen powder was resuspended in 300 µl of methanol containing 1 % HCl. After vortex-mixing for 15 sec, cell debris was pelleted by centrifugation for 15 min at >14,000 g, 4°C. The supernatant was mixed with 200 µl water and 500 µl chloroform by vortexing for 15 sec. After 15 min centrifugation at 17,900 g, 4°C, the upper phase was diluted in methanol to measure the absorbance at 535 nm and 630 nm using a spectrophotometer (Specord 200 Plus, Analytik Jena, Jena, Germany).

Measurements of starch, soluble sugars, and adenylates

Carbohydrates were determined by the Warburg optical test and adenylates were assessed based on luciferase activity. Both procedures were described previously (Mustroph et al., 2006), for details see supplemental methods.

Determination of P_i contents

Free P_i was determined in leaf tissue based on the method described by (Ames, 1966) with some modifications partially based on (Sakuraba et al., 2018). For detail see supplemental methods.

RNA extraction and cDNA synthesis

Plant material was harvested under the respective experimental conditions and instantly frozen in liquid nitrogen. The tissue was ground in a bead mill, and RNA was extracted using Bioline TRIsure (Meridian Bioscience, Cincinnati, United States) according to the manufacturer's instructions. The quality of the RNA was assessed by screening A_{260} and A_{280}. For qRT-PCR analysis, 1 µg of RNA was treated with DNAse I (Thermo Fisher Scientific, Waltham, United States) according to product instructions before application in reverse

596 transcription using oligo(dT)$_{15}$ and RevertAid Reverse Transcriptase (Thermo Fisher
597 Scientific). Complementary DNA was diluted by a factor of 50 for use as template in qPCR
598 analysis. qPCR was performed in technical triplicates using SsoAdvanced Universal SYBR
599 Green Supermix (Bio-Rad, Hercules, United States) on a CFX Connect Real-time System (Bio-
600 Rad). Transcript levels were normalized to the levels of *PP2A* transcript and calculated as
601 $1000 \cdot 2^{-\Delta CT}$. Primer sequences are listed in table S1.

602

603 **Protoplast isolation, transfection and transactivation assay**

604 Leaf mesophyll protoplasts were isolated using the "Tape-Arabidopsis Sandwich"
605 method (Wu et al., 2009) with minor modifications. For details, see supplemental methods.

606

607 **Chlorophyll fluorescence measurements**

608 For the determination of the quantum yield of photosystem II photochemistry
609 (F_m'-F')/F_m' (ΦPSII), as well as the maximum efficiency of photosystem II (F_v'/F_m'), pulse-
610 amplitude-modulated fluorescence measurements (PAM) of chlorophyll fluorescence were
611 conducted using a Junior-PAM (Walz, Effeltrich, Germany). Here, to calculate chlorophyll
612 fluorescence parameters using the saturating pulse method (Schreiber et al., 1986), one large
613 rosette leaf was held between two magnets and subjected to 10 seconds of actinic light
614 irradiance set to control light intensity (80±5 µmol m^{-2} sec^{-1}), followed by a saturation light
615 pulse.

616

617 **Statistical analysis**

618 Statistical analyses were performed with Microsoft Office Excel using the Real
619 Statistics Resource Pack software (www.real-statistics.com).

620

621 # Funding information

622 This research was funded by the University of Bayreuth.

Acknowledgements

We thank Stephan Clemens and Angelika Mustroph for helpful discussions and comments on the manuscript, as well as for providing infrastructure and equipment. We thank Kristina Munzert for help with experiments.

Author contributions

M. K. designed the research, analyzed data, and wrote the paper; L. A., M. M., A. H., and M. K. performed research.

Supplemental Data

Supplemental Figure 1 Changes in sugar and starch contents under P_i depletion.

Supplemental Figure 2 Expression of selected P_i-starvation responsive genes is activated by PHR1/PHL1.

Supplemental Figure 3 *PHR1* transcript levels are not affected by short-time high-light exposure.

Supplemental Figure 4 Anthocyanin production of P_i signaling mutants under ROS stress.

Supplemental Figure 5 Delayed onset of flowering in *phr1-1 phl1* mutants.

Supplemental Figure 6 Quantification of shoot fresh weights of seedlings grown under low and high light.

Supplemental Figure 7 Root growth of *adg1 phr1 phl1* and *adg1 tpt-2* responds to exogenously supplied sucrose.

Supplemental Figure 8 Carbohydrate responsive gene expression is affected under P_i starvation.

Supplemental Table 1 List of primer sequences used in this study.

Supplemental Methods

REFERENCES

Aleksza D, Horváth G V., Sándor G, Szabados L (2017) Proline accumulation is regulated by transcription factors associated with phosphate starvation. Plant Physiol **175**: 555–567

Ames BN (1966) [10] Assay of inorganic phosphate, total phosphate and phosphatases. Methods Enzymol. pp 115–118

Athanasiou K, Dyson BC, Webster RE, Johnson GN (2010) Dynamic acclimation of photosynthesis increases plant fitness in changing environments. Plant Physiol **152**: 366–73

Baena-González E, Rolland F, Thevelein JM, Sheen J (2007) A central integrator of transcription networks in plant stress and energy signalling. Nature **448**: 938–42

Barragán-Rosillo AC, Peralta-Alvarez CA, Ojeda-Rivera JO, Arzate-Mejía RG, Recillas-Targa F, Herrera-Estrella L (2021) Genome accessibility dynamics in response to phosphate limitation is controlled by the PHR1 family of transcription factors in Arabidopsis. Proc Natl Acad Sci U S A **118**: e2107558118

Bäumler J, Riber W, Klecker M, Müller L, Dissmeyer N, Weig AR, Mustroph A (2019) AtERF#111/ABR1 is a transcriptional activator involved in the wounding response. Plant J **100**: 969–990

Bechtold U, Richard O, Zamboni A, Gapper C, Geisler M, Pogson B, Karpinski S, Mullineaux PM (2008) Impact of chloroplastic- and extracellular-sourced ROS on high light-responsive gene expression in Arabidopsis. J Exp Bot **59**: 121–33

Bläsing OE, Gibon Y, Günther M, Höhne M, Morcuende R, Osuna D, Thimm O, Usadel B, Scheible W-R, Stitt M (2005) Sugars and circadian regulation make major contributions to the global regulation of diurnal gene expression in Arabidopsis. Plant Cell **17**: 3257–81

Bustos R, Castrillo G, Linhares F, Puga MI, Rubio V, Pérez-Pérez J, Solano R, Leyva A, Paz-Ares J (2010) A central regulatory system largely controls transcriptional activation and repression responses to phosphate starvation in Arabidopsis. PLoS Genet **6**: e1001102

Castrillo G, Teixeira PJPL, Paredes SH, Law TF, de Lorenzo L, Feltcher ME, Finkel OM, Breakfield NW, Mieczkowski P, Jones CD, et al (2017) Root microbiota drive direct integration of phosphate stress and immunity. Nature **543**: 513–518

Cheng Y, Zhou W, El Sheery NI, Peters C, Li M, Wang X, Huang J (2011) Characterization

of the Arabidopsis glycerophosphodiester phosphodiesterase (GDPD) family reveals a role of the plastid-localized AtGDPD1 in maintaining cellular phosphate homeostasis under phosphate starvation. Plant J **66**: 781–95

Dietz K-J (2015) Efficient high light acclimation involves rapid processes at multiple mechanistic levels. J Exp Bot **66**: 2401–14

Dietz K-J, Heber U (1986) Light and CO2 limitation of photosynthesis and states of the reactions regenerating ribulose 1,5-bisphosphate or reducing 3-phosphoglycerate. Biochim Biophys Acta - Bioenerg **848**: 392–401

Dietz K-J, Turkan I, Krieger-Liszkay A (2016) Redox- and Reactive Oxygen Species-Dependent Signaling into and out of the Photosynthesizing Chloroplast. Plant Physiol **171**: 1541–50

Dietz K, Heber U (1984) Rate-limiting factors in leaf photosynthesis. I. Carbon fluxes in the calvin cycle. Biochim Biophys Acta - Bioenerg **767**: 432–443

Dietz KJ, Foyer C (1986) The relationship between phosphate status and photosynthesis in leaves : Reversibility of the effects of phosphate deficiency on photosynthesis. Planta **167**: 376–81

Dong J, Ma G, Sui L, Wei M, Satheesh V, Zhang R, Ge S, Li J, Zhang T-E, Wittwer C, et al (2019) Inositol Pyrophosphate InsP8 Acts as an Intracellular Phosphate Signal in Arabidopsis. Mol Plant **12**: 1463–1473

Fabiańska I, Bucher M, Häusler RE (2019) Intracellular phosphate homeostasis - A short way from metabolism to signaling. Plant Sci **286**: 57–67

Figueroa CM, Asencion Diez MD, Ballicora MA, Iglesias AA (2022) Structure, function, and evolution of plant ADP-glucose pyrophosphorylase. Plant Mol Biol **108**: 307–323

Frank A, Matiolli CC, Viana AJC, Hearn TJ, Kusakina J, Belbin FE, Wells Newman D, Yochikawa A, Cano-Ramirez DL, Chembath A, et al (2018) Circadian Entrainment in Arabidopsis by the Sugar-Responsive Transcription Factor bZIP63. Curr Biol **28**: 2597-2606.e6

Hammond JP, White PJ (2008) Sucrose transport in the phloem: integrating root responses to phosphorus starvation. J Exp Bot **59**: 93–109

Hanchi M, Thibaud M-C, Légeret B, Kuwata K, Pochon N, Beisson F, Cao A, Cuyas L, David P, Doerner P, et al (2018) The Phosphate Fast-Responsive Genes PECP1 and

711 PPsPase1 Affect Phosphocholine and Phosphoethanolamine Content. Plant Physiol **176**:
712 2943–2962

713 **Härtel H, Dormann P, Benning C** (2000) DGD1-independent biosynthesis of extraplastidic
714 galactolipids after phosphate deprivation in Arabidopsis. Proc Natl Acad Sci U S A **97**:
715 10649–54

716 **Häusler RE, Heinrichs L, Schmitz J, Flügge UI** (2014) How sugars might coordinate
717 chloroplast and nuclear gene expression during acclimation to high light intensities. Mol
718 Plant **7**: 1121–1137

719 **Heinrichs L, Schmitz J, Flügge U-I, Häusler RE** (2012) The Mysterious Rescue of adg1-
720 1/tpt-2 - an Arabidopsis thaliana Double Mutant Impaired in Acclimation to High Light -
721 by Exogenously Supplied Sugars. Front Plant Sci **3**: 265

722 **Heldt HW, Rapley L** (1970) Specific transport of inorganic phosphate, 3-phosphoglycerate
723 and dihydroxyacetonephosphate, and of dicarboxylates across the inner membrane of
724 spinach chloroplasts. FEBS Lett **10**: 143–148

725 **Hendriks JHM, Kolbe A, Gibon Y, Stitt M, Geigenberger P** (2003) ADP-glucose
726 pyrophosphorylase is activated by posttranslational redox-modification in response to light
727 and to sugars in leaves of Arabidopsis and other plant species. Plant Physiol **133**: 838–49

728 **Hilgers EJA, Schöttler MA, Mettler-Altmann T, Krueger S, Dörmann P, Eicks M, Flügge**
729 **UI, Häusler RE** (2018) The combined loss of triose phosphate and xylulose 5-
730 phosphate/phosphate translocators leads to severe growth retardation and impaired
731 photosynthesis in arabidopsis thaliana tpt/xpt double mutants. Front Plant Sci **9**: 1–24

732 **Huang J, Zhao X, Chory J** (2019) The Arabidopsis Transcriptome Responds Specifically and
733 Dynamically to High Light Stress. Cell Rep **29**: 4186-4199.e3

734 **Klecker M, Gasch P, Peisker H, Dörmann P, Schlicke H, Grimm B, Mustroph A** (2014) A
735 Shoot-Specific Hypoxic Response of Arabidopsis Sheds Light on the Role of the
736 Phosphate-Responsive Transcription Factor PHOSPHATE STARVATION
737 RESPONSE1. Plant Physiol **165**: 774–790

738 **Kobayashi K, Awai K, Takamiya K, Ohta H** (2004) Arabidopsis type B
739 monogalactosyldiacylglycerol synthase genes are expressed during pollen tube growth and
740 induced by phosphate starvation. Plant Physiol **134**: 640–8

741 **König J, Muthuramalingam M, Dietz K-J** (2012) Mechanisms and dynamics in the

742 thiol/disulfide redox regulatory network: transmitters, sensors and targets. Curr Opin Plant
743 Biol **15**: 261–8

744 **Kumar V, Sharma A, Bhardwaj R, Thukral AK** (2019) Elemental Composition of Plants
745 and Multivariate Analysis. Natl Acad Sci Lett **42**: 45–50

746 **Kunz HH, Häusler RE, Fettke J, Herbst K, Niewiadomski P, Gierth M, Bell K, Steup M,**
747 **Flügge U-I, Schneider A** (2010) The role of plastidial glucose-6-phosphate/phosphate
748 translocators in vegetative tissues of Arabidopsis thaliana mutants impaired in starch
749 biosynthesis. Plant Biol (Stuttg) **12 Suppl 1**: 115–28

750 **Laisk A, Siebke K, Gerst U, Eichelmann H, Oja V, Heber U** (1991) Oscillations in
751 photosynthesis are initiated and supported by imbalances in the supply of ATP and
752 NADPH to the Calvin cycle. Planta **185**: 554–62

753 **Lei M, Liu Y, Zhang B, Zhao Y, Wang X, Zhou Y, Raghothama KG, Liu D** (2011) Genetic
754 and genomic evidence that sucrose is a global regulator of plant responses to phosphate
755 starvation in Arabidopsis. Plant Physiol **156**: 1116–30

756 **Li H, He K, Zhang Z, Hu Y** (2023) Molecular mechanism of phosphorous signaling inducing
757 anthocyanin accumulation in Arabidopsis. Plant Physiol Biochem **196**: 121–129

758 **Lin TP, Caspar T, Somerville C, Preiss J** (1988) Isolation and Characterization of a
759 Starchless Mutant of Arabidopsis thaliana (L.) Heynh Lacking ADPglucose
760 Pyrophosphorylase Activity. Plant Physiol **86**: 1131–5

761 **Liu Y, Xie Y, Wang H, Ma X, Yao W, Wang H** (2017) Light and ethylene coordinately
762 regulate the phosphate starvation response through transcriptional regulation of
763 PHOSPHATE STARVATION RESPONSE1. Plant Cell **29**: 2269–2284

764 **Liu Z, Wu X, Wang E, Liu Y, Wang Y, Zheng Q, Han Y, Chen Z, Zhang Y** (2022) PHR1
765 positively regulates phosphate starvation-induced anthocyanin accumulation through
766 direct upregulation of genes F3'H and LDOX in Arabidopsis. Planta **256**: 42

767 **MacNeill GJ, Mehrpouyan S, Minow MAA, Patterson JA, Tetlow IJ, Emes MJ** (2017)
768 Starch as a source, starch as a sink: the bifunctional role of starch in carbon allocation. J
769 Exp Bot **68**: 4433–4453

770 **Matiolli CC, Soares RC, Alves HLS, Abreu IA** (2022) Turning the Knobs: The Impact of
771 Post-translational Modifications on Carbon Metabolism. Front Plant Sci **12**: 781508

772 **Matiolli CC, Tomaz JP, Duarte GT, Prado FM, Del Bem LEV, Silveira AB, Gauer L,**

Corrêa LGG, Drumond RD, Viana AJC, et al (2011) The Arabidopsis bZIP gene AtbZIP63 is a sensitive integrator of transient abscisic acid and glucose signals. Plant Physiol **157**: 692–705

Matsoukas IG, Massiah AJ, Thomas B (2013) Starch metabolism and antiflorigenic signals modulate the juvenile-to-adult phase transition in Arabidopsis. Plant Cell Environ **36**: 1802–11

Maxwell K, Johnson GN (2000) Chlorophyll fluorescence--a practical guide. J Exp Bot **51**: 659–68

Misson J, Raghothama KG, Jain A, Jouhet J, Block MA, Bligny R, Ortet P, Creff A, Somerville S, Rolland N, et al (2005) A genome-wide transcriptional analysis using Arabidopsis thaliana Affymetrix gene chips determined plant responses to phosphate deprivation. Proc Natl Acad Sci U S A **102**: 11934–9

Moore M, Vogel MO, Dietz KJ (2014) The acclimation response to high light is initiated within seconds as indicated by upregulation of AP2/ERF transcription factor network in Arabidopsis thaliana. Plant Signal Behav **9**: 1–4

Morcuende R, Bari R, Gibon Y, Zheng W, Pant BD, Bläsing O, Usadel B, Czechowski T, Udvardi MK, Stitt M, et al (2007) Genome-wide reprogramming of metabolism and regulatory networks of Arabidopsis in response to phosphorus. Plant Cell Environ **30**: 85–112

Mustroph A, Boamfa EI, Laarhoven LJJ, Harren FJM, Albrecht G, Grimm B (2006) Organ-specific analysis of the anaerobic primary metabolism in rice and wheat seedlings. I: Dark ethanol production is dominated by the shoots. Planta **225**: 103–14

Nam H-I, Shahzad Z, Dorone Y, Clowez S, Zhao K, Bouain N, Lay-Pruitt KS, Cho H, Rhee SY, Rouached H (2021) Interdependent iron and phosphorus availability controls photosynthesis through retrograde signaling. Nat Commun **12**: 7211

Niewiadomski P, Knappe S, Geimer S, Fischer K, Schulz B, Unte US, Rosso MG, Ache P, Flügge UI, Schneider A (2005) The Arabidopsis plastidic glucose 6-phosphate/phosphate translocator GPT1 is essential for pollen maturation and embryo sac development. Plant Cell **17**: 760–775

Nilsson L, Lundmark M, Jensen PE, Nielsen TH (2012) The Arabidopsis transcription factor PHR1 is essential for adaptation to high light and retaining functional photosynthesis during phosphate starvation. Physiol Plant **144**: 35–47

805 **Nilsson L, Müller R, Nielsen TH** (2007) Increased expression of the MYB-related
806 transcription factor, PHR1, leads to enhanced phosphate uptake in Arabidopsis thaliana.
807 Plant Cell Environ **30**: 1499–512

808 **Ohnishi M, Anegawa A, Sugiyama Y, Harada K, Oikawa A, Nakayama Y, Matsuda F,**
809 **Nakamura Y, Sasaki R, Shichijo C, et al** (2018) Molecular Components of Arabidopsis
810 Intact Vacuoles Clarified with Metabolomic and Proteomic Analyses. Plant Cell Physiol
811 **59**: 1353–1362

812 **Osorio MB, Ng S, Berkowitz O, De Clercq I, Mao C, Shou H, Whelan J, Jost R** (2019)
813 SPX4 Acts on PHR1-Dependent and -Independent Regulation of Shoot Phosphorus Status
814 in Arabidopsis. Plant Physiol **181**: 332–352

815 **Pant B-D, Pant P, Erban A, Huhman D, Kopka J, Scheible W-R** (2015a) Identification of
816 primary and secondary metabolites with phosphorus status-dependent abundance in
817 Arabidopsis, and of the transcription factor PHR1 as a major regulator of metabolic
818 changes during phosphorus limitation. Plant Cell Environ **38**: 172–87

819 **Pant BD, Burgos A, Pant P, Cuadros-Inostroza A, Willmitzer L, Scheible WR** (2015b) The
820 transcription factor PHR1 regulates lipid remodeling and triacylglycerol accumulation in
821 Arabidopsis thaliana during phosphorus starvation. J Exp Bot **66**: 1907–1918

822 **Paz-Ares J, Puga MI, Rojas-Triana M, Martinez-Hevia I, Diaz S, Poza-Carrión C,**
823 **Miñambres M, Leyva A** (2022) Plant adaptation to low phosphorus availability: Core
824 signaling, crosstalks, and applied implications. Mol Plant **15**: 104–124

825 **Preiss J** (1984) Starch, sucrose biosynthesis and partition of carbon in plants are regulated by
826 orthophosphate and triose-phosphates. Trends Biochem Sci **9**: 24–27

827 **Preiss J** (1988) Biosynthesis of starch and its regulation. *In* J Preiss, ed, Biochem. Plants, 14th
828 ed. Academic Press, San Diego, pp 181–254

829 **Puga MI, Mateos I, Charukesi R, Wang Z, Franco-Zorrilla JM, de Lorenzo L, Irigoyen**
830 **ML, Masiero S, Bustos R, Rodríguez J, et al** (2014) SPX1 is a phosphate-dependent
831 inhibitor of Phosphate Starvation Response 1 in Arabidopsis. Proc Natl Acad Sci U S A
832 **111**: 14947–52

833 **Ramaiah M, Jain A, Baldwin JC, Karthikeyan AS, Raghothama KG** (2011)
834 Characterization of the phosphate starvation-induced glycerol-3-phosphate permease gene
835 family in Arabidopsis. Plant Physiol **157**: 279–91

Rawat R, Schwartz J, Jones MA, Sairanen I, Cheng Y, Andersson CR, Zhao Y, Ljung K, Harmer SL (2009) REVEILLE1, a Myb-like transcription factor, integrates the circadian clock and auxin pathways. Proc Natl Acad Sci U S A **106**: 16883–8

Ried MK, Wild R, Zhu J, Pipercevic J, Sturm K, Broger L, Harmel RK, Abriata LA, Hothorn LA, Fiedler D, et al (2021) Inositol pyrophosphates promote the interaction of SPX domains with the coiled-coil motif of PHR transcription factors to regulate plant phosphate homeostasis. Nat Commun **12**: 384

Riemer E, Qiu D, Laha D, Harmel RK, Gaugler P, Gaugler V, Frei M, Hajirezaei M-R, Laha NP, Krusenbaum L, et al (2021) ITPK1 is an InsP6/ADP phosphotransferase that controls phosphate signaling in Arabidopsis. Mol Plant **14**: 1864–1880

Robinson S, Giersch C (1987) Inorganic Phosphate Concentration in the Stroma of Isolated Chloroplasts and Its Influence on Photosynthesis. Aust J Plant Physiol **14**: 451

van Rooijen R, Harbinson J, Aarts MGM (2018) Photosynthetic response to increased irradiance correlates to variation in transcriptional response of lipid-remodeling and heat-shock genes. Plant direct **2**: e00069

Rubio V, Linhares F, Solano R, Martín AC, Iglesias J, Leyva A, Paz-Ares J (2001) A conserved MYB transcription factor involved in phosphate starvation signaling both in vascular plants and in unicellular algae. Genes Dev **15**: 2122–33

Sakuraba Y, Kanno S, Mabuchi A, Monda K, Iba K, Yanagisawa S (2018) A phytochrome-B-mediated regulatory mechanism of phosphorus acquisition. Nat plants **4**: 1089–1101

Scheible W-R, Pant P, Pant BD, Krom N, Allen RD, Mysore KS (2023) Elucidating the unknown transcriptional responses and PHR1 mediated biotic and abiotic stress tolerance during phosphorus-limitation. J Exp Bot **11**: erad009

Schmitz J, Schöttler MA, Krueger S, Geimer S, Schneider A, Kleine T, Leister D, Bell K, Flügge U-I, Häusler RE (2012) Defects in leaf carbohydrate metabolism compromise acclimation to high light and lead to a high chlorophyll fluorescence phenotype in Arabidopsis thaliana. BMC Plant Biol **12**: 8

Schneider A, Häusler RE, Kolukisaoglu Ü, Kunze R, Van der Graaff E, Schwacke R, Catoni E, Desimone M, Flügge UI (2002) An Arabidopsis thaliana knock-out mutant of the chloroplast triose phosphate/phosphate translocator is severely compromised only when starch synthesis, but not starch mobilisation is abolished. Plant J **32**: 685–699

867 **Schreiber U, Schliwa U, Bilger W** (1986) Continuous recording of photochemical and non-
868 photochemical chlorophyll fluorescence quenching with a new type of modulation
869 fluorometer. Photosynth Res **10**: 51–62

870 **Sivak MN, Walker DA** (1986) Photosynthesis in vivo can be limited by phosphate supply.
871 New Phytol **102**: 499–512

872 **Smith AM, Stitt M** (2007) Coordination of carbon supply and plant growth. Plant Cell Environ
873 **30**: 1126–49

874 **Stitt M, Grosse H** (1988) Interactions between Sucrose Synthesis and CO2 Fixation IV.
875 Temperature-dependent adjustment of the relation between sucrose synthesis and CO2
876 fixation. J Plant Physiol **133**: 392–400

877 **Stitt M, Wirtz W, Heldt HW** (1980) Metabolite levels during induction in the chloroplast and
878 extrachloroplast compartments of spinach protoplasts. Biochim Biophys Acta **593**: 85–
879 102

880 **Stitt M, Wirtz W, Heldt HW** (1983) Regulation of Sucrose Synthesis by Cytoplasmic
881 Fructosebisphosphatase and Sucrose Phosphate Synthase during Photosynthesis in
882 Varying Light and Carbon Dioxide. Plant Physiol **72**: 767–74

883 **Sun L, Song L, Zhang Y, Zheng Z, Liu D** (2016) Arabidopsis PHL2 and PHR1 Act
884 Redundantly as the Key Components of the Central Regulatory System Controlling
885 Transcriptional Responses to Phosphate Starvation. Plant Physiol **170**: 499–514

886 **Suzuki N, Devireddy AR, Inupakutika MA, Baxter A, Miller G, Song L, Shulaev E, Azad**
887 **RK, Shulaev V, Mittler R** (2015) Ultra-fast alterations in mRNA levels uncover multiple
888 players in light stress acclimation in plants. Plant J **84**: 760–72

889 **Thibaud M-C, Arrighi J-F, Bayle V, Chiarenza S, Creff A, Bustos R, Paz-Ares J, Poirier**
890 **Y, Nussaume L** (2010) Dissection of local and systemic transcriptional responses to
891 phosphate starvation in Arabidopsis. Plant J **64**: 775–89

892 **Vandenbussche F, Habricot Y, Condiff AS, Maldiney R, Van Der Straeten D, Ahmad M**
893 (2007) HY5 is a point of convergence between cryptochrome and cytokinin signalling
894 pathways in Arabidopsis thaliana. Plant J **49**: 428–441

895 **Vogel MO, Moore M, König K, Pecher P, Alsharafa K, Lee J, Dietz KJ** (2014) Fast
896 retrograde signaling in response to high light involves metabolite export, MITOGEN-
897 ACTIVATED PROTEIN KINASE6, and AP2/ERF transcription factors in Arabidopsis.

Plant Cell **26**: 1151–1165

Wahl V, Ponnu J, Schlereth A, Arrivault S, Langenecker T, Franke A, Feil R, Lunn JE, Stitt M, Schmid M (2013) Regulation of flowering by trehalose-6-phosphate signaling in Arabidopsis thaliana. Science **339**: 704–7

Wang Z, Zheng Z, Song L, Liu D (2018a) Functional Characterization of Arabidopsis PHL4 in Plant Response to Phosphate Starvation. Front Plant Sci **9**: 1432

Wang ZQ, Zhou X, Dong L, Guo J, Chen Y, Zhang Y, Wu L, Xu M (2018b) iTRAQ-based analysis of the Arabidopsis proteome reveals insights into the potential mechanisms of anthocyanin accumulation regulation in response to phosphate deficiency. J Proteomics **184**: 39–53

Ward JT, Lahner B, Yakubova E, Salt DE, Raghothama KG (2008) The effect of iron on the primary root elongation of Arabidopsis during phosphate deficiency. Plant Physiol **147**: 1181–91

Weise SE, Liu T, Childs KL, Preiser AL, Katulski HM, Perrin-Porzondek C, Sharkey TD (2019) Transcriptional Regulation of the Glucose-6-Phosphate/Phosphate Translocator 2 Is Related to Carbon Exchange Across the Chloroplast Envelope. Front Plant Sci **10**: 827

Woodrow IE, Raymond Ellis J, Jellings A, Foyer CH (1984) Compartmentation and fluxes of inorganic phosphate in photosynthetic cells. Planta **161**: 525–30

Wu FH, Shen SC, Lee LY, Lee SH, Chan MT, Lin CS (2009) Tape-arabidopsis sandwich - A simpler arabidopsis protoplast isolation method. Plant Methods **5**: 1–10

Xu L, Zhao H, Wan R, Liu Y, Xu Z, Tian W, Ruan W, Wang F, Deng M, Wang J, et al (2019) Identification of vacuolar phosphate efflux transporters in land plants. Nat plants **5**: 84–94

Yu L, Fan J, Zhou C, Xu C (2021) Chloroplast lipid biosynthesis is fine-tuned to thylakoid membrane remodeling during light acclimation. Plant Physiol **185**: 94–107

Zhou J, Jiao F, Wu Z, Li Y, Wang X, He X, Zhong W, Wu P (2008) OsPHR2 is involved in phosphate-starvation signaling and excessive phosphate accumulation in shoots of plants. Plant Physiol **146**: 1673–86

Zhu J, Lau K, Puschmann R, Harmel RK, Zhang Y, Pries V, Gaugler P, Broger L, Dutta AK, Jessen HJ, et al (2019) Two bifunctional inositol pyrophosphate kinases/phosphatases control plant phosphate homeostasis. Elife **8**: 1–25

929 **Zirngibl M-E, Araguirang GE, Kitashova A, Jahnke K, Rolka T, Kühn C, Nägele T,**
930 **Richter AS** (2023) Triose phosphate export from chloroplasts and cellular sugar content
931 regulate anthocyanin biosynthesis during high light acclimation. Plant Commun **4**: 100423

932

933

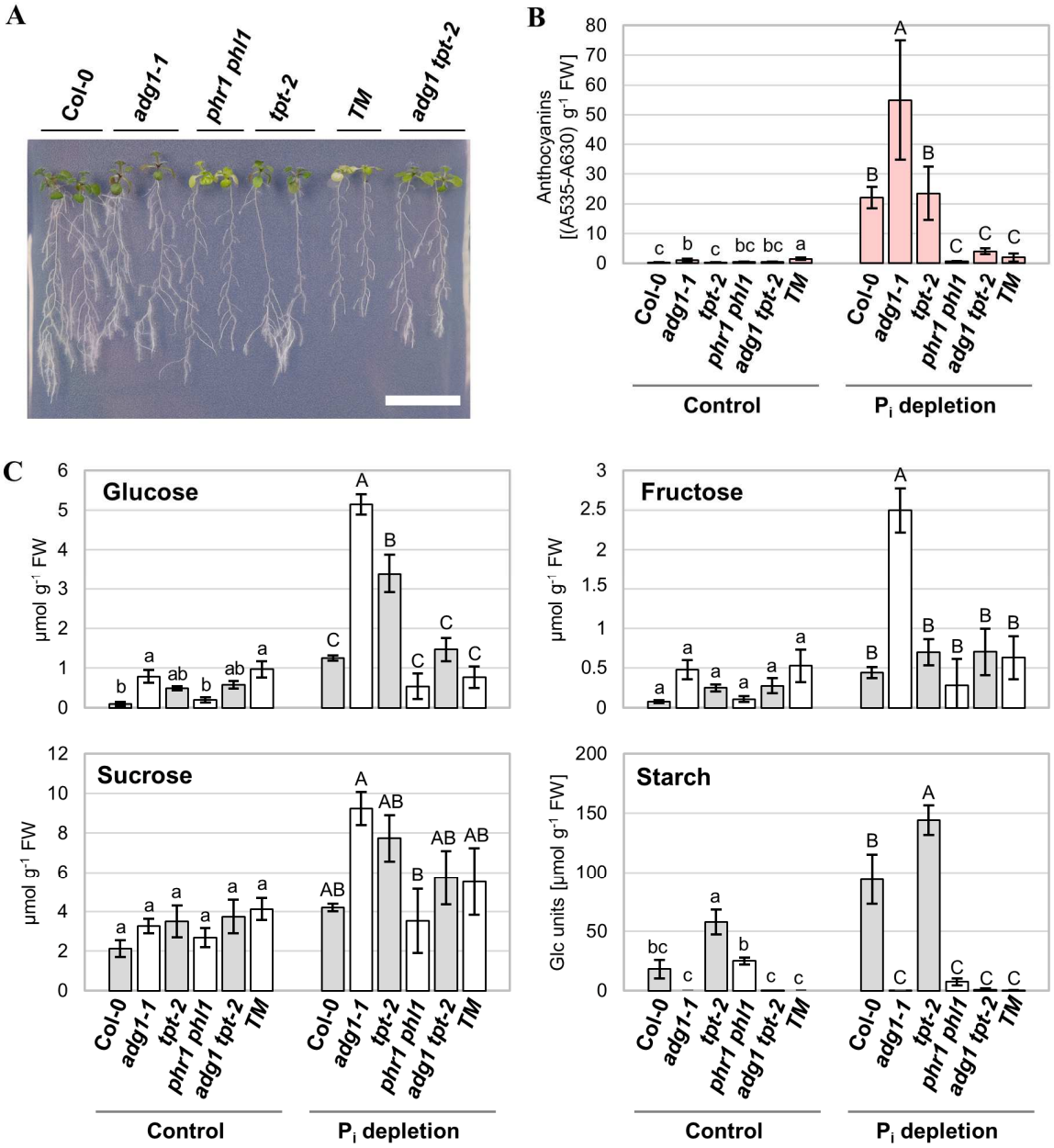

Figure 1 P_i starvation responses are affected by photoassimilate partitioning. **A-C,** Seedlings of wildtype (Col-0), *adg1-1*, *tpt-2*, *phr1-3 phl1*, *adg1 tpt-2* and *adg1 phr1-3 phl1* (**TM**) genotype were grown for 7 (A), 5 (B), or 10 (C) days on rich medium including 0.5 % sucrose before transfer to media with 0.5 % sucrose and either 2.5 mM (**Control**) or 0 mM (**P_i depletion**) KH_2PO_4 added. Growth was continued for 8 (A), or 7 (B, C) days. **A,** Seedling phenotypes under P_i deficient growth conditions. Bar, 2 cm. **B,** Anthocyanin contents of seedling shoots. Pigment levels are depicted as units of absorbance (A535 - A630) relative to shoot fresh weights. Bars represent means ± standard deviations; *n* = 5-6 pools of seedling shoots from 3 independent experiments; **C,** Contents of glucose, fructose, sucrose and starch. Pools of seedling shoots were harvested 10.25 hours after onset of the 16-hours photoperiod.

945 Means ± standard deviations; $n = 3$ independent experiments. **B, C,** Statistical analyses were
946 performed with One-way ANOVA with Tukey HSD follow-up test and Bonferroni alpha
947 correction for contrasts; $P < 0.05$.

948

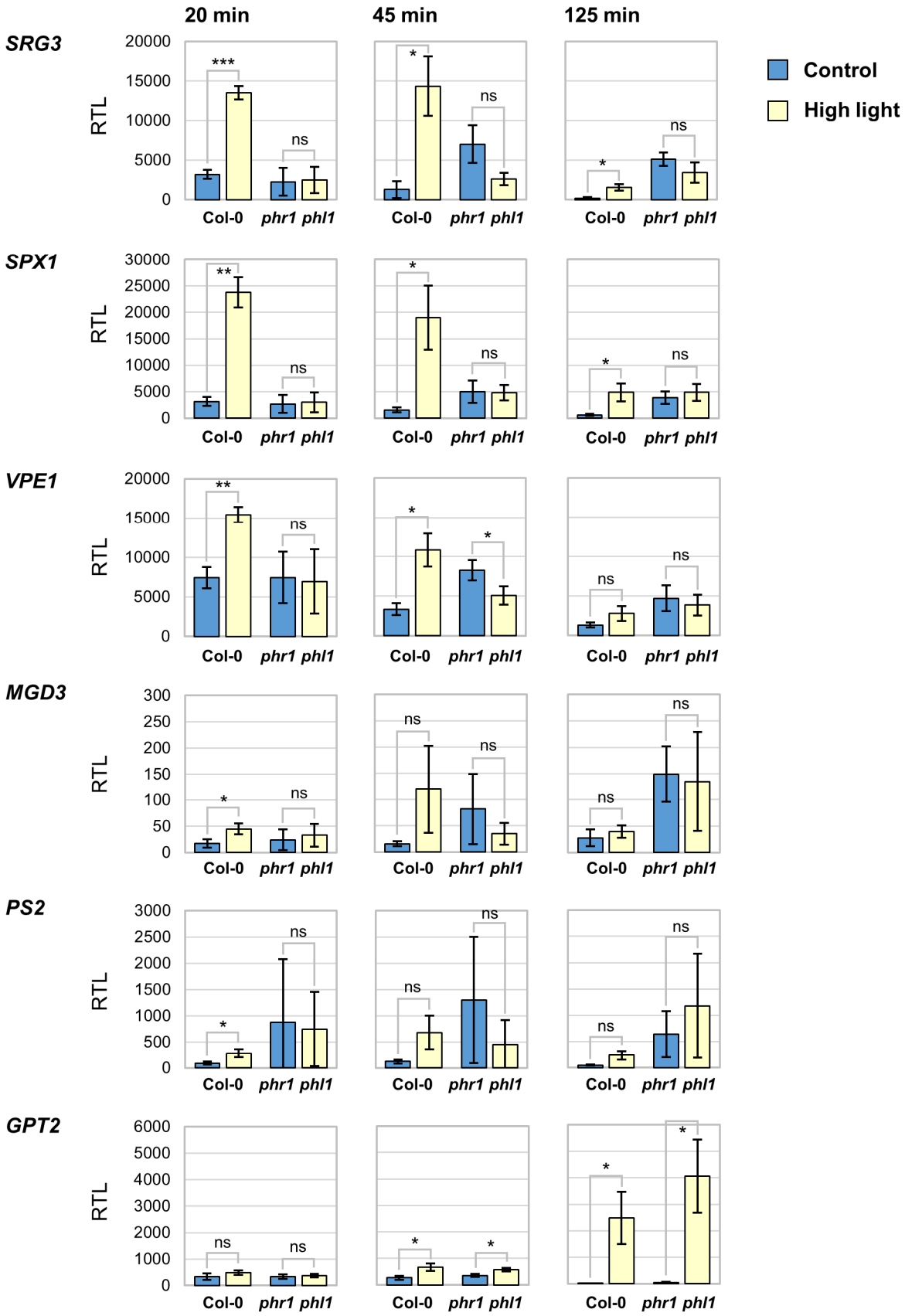

Figure 2 PHR1-target genes are rapidly induced by high light. qRT-PCR analyses of indicated transcripts in rosette leaves from wildtype (Col-0) and *phr1-1 phl1* mutants. Plants were grown on soil for 5 weeks in an 8-hours light regime at 80±5 µmol m^{-2} s^{-1} before light intensity was

953 set to 320±30 µmol m^{-2} s^{-1} (High light, yellow bars) starting 1 hour after onset of the
954 photoperiod on day 36. The control group was kept at 80±5 µmol m^{-2} s^{-1} (blue bars). Per sample,
955 2-3 fully developed leaves (leaves no. 10-13) were harvested at the indicated treatment times.
956 Transcript levels were calculated relative to *PP2A* as $1000 \cdot 2^{-\Delta CT}$. Bars represent means
957 ± standard deviations, $n = 3$ independent experiments. Statistical analyses were performed
958 using Student's *t* test with 2-tailed distribution, unpaired with unequal variance. Significant
959 differences are indicated as ***P <0.001, **P <0.01, *P <0.05, ns, not significant.

960

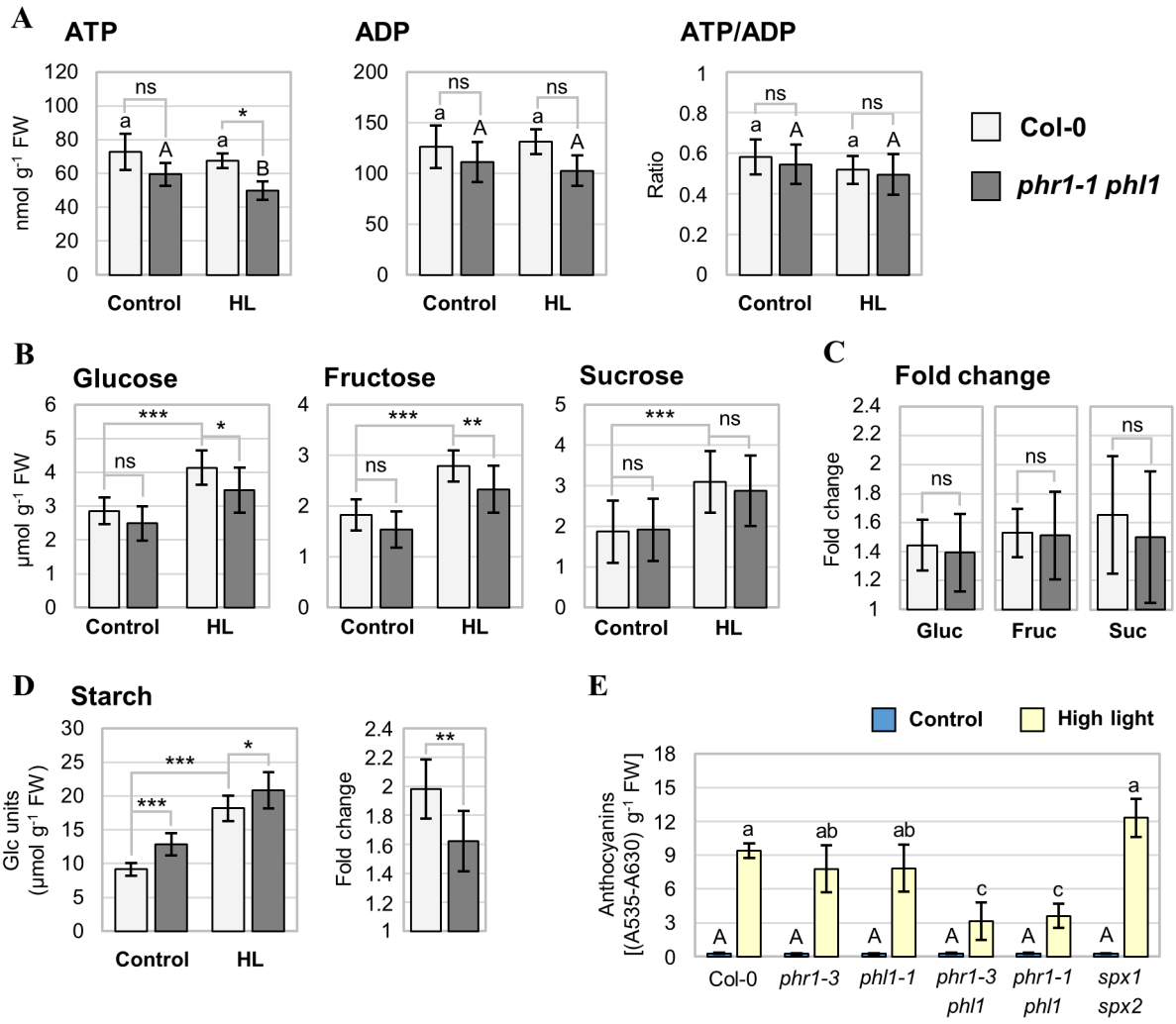

Figure 3 High-light induced metabolic changes in *phr1-1 phl1*. **A-D,** Levels of the indicated metabolites in leaves of wildtype (Col-0, light grey bars) and *phr1-1 phl1* mutants (dark grey bars) are depicted. Plants were grown and treated as described in Figure 2. Fully expanded leaves were sampled after 90 min of exposure to a photon flux density of either 80±5 µmol m^{-2} s^{-1} (**Control**) or 320±30 µmol m^{-2} s^{-1} (**HL**). Bars show means ± standard deviations; statistical analyses were performed with Student's *t* test with two-tailed distribution, unpaired with unequal variance. Significant differences are indicated as *** P <0.001, ** P <0.01, * P <0.05, ns not significant. **A,** n = 6 plants from 3 independent experiments; significant differences indicated by letter code: P <0.05. **B, C,** n = 11-12 plants from 4 independent experiments. **C, D,** Fold changes of sugar/starch contents were calculated for each genotype as HL/mean of control. **Gluc** glucose; **Fruc** fructose; **Suc** sucrose. **D,** n = 9 plants from 3 independent experiments. **E,** Anthocyanin levels determined in leaves of the indicated genotypes after 3 days of high-light exposure. Plants were grown for 32 days under low light conditions (70±10 µmol m^{-2} s^{-1}) in an 8-hours light regime. Subsequently, light intensity was increased for the treatment group (High light, yellow bars) to 450±30 µmol m^{-2} s^{-1}, while the

977 control group (blue bars) was kept under growth light conditions. Leaf material was harvested
978 after additional 70 hours. Pigment contents are expressed as absorbance units (A535 - A630)
979 relative to shoot fresh weight. n = 3 independent experiments; statistical analyses were
980 conducted using One-way ANOVA with Tukey HSD follow-up test and Bonferroni alpha
981 correction for contrasts, P <0.01; ns, not significant.

982

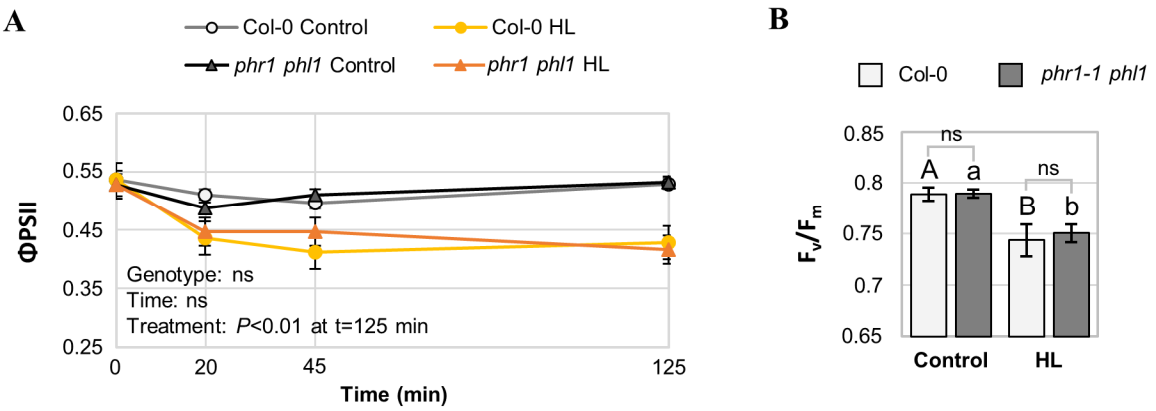

983

984 **Figure 4** Effect of high light on chlorophyll fluorescence in the *phr1-1 phl1* mutant. Plants of
985 wildtype (Col-0) and *phr1-1 phl1* genotype were grown as described in Figure 2. After 5 weeks
986 of growth, the light intensity was increased to 320±30 µmol m^{-2} s^{-1} for high-light (**HL**)
987 treatments, whereas the control group was kept under growth light conditions
988 (80±5 µmol m^{-2} s^{-1}). n = 3 independent experiments (representing means of each 3 leaves
989 measured). Significance was tested using One-way ANOVA with Tukey HSD follow-up test
990 and Bonferroni alpha correction for contrasts; ns, not significant. **A,** PAM measurements were
991 performed to determine the quantum yield of photosystem II photochemistry (ΦPSII) on light-
992 adapted leaves after 20, 45, and 125 min of treatment. **B,** Plants subjected to high-light stress
993 were dark-adapted for 20 min after 125 min of stress duration to determine the maximum
994 efficiency of photosystem II (F_v/F_m). Bars show means ± standard deviations; P <0.01.

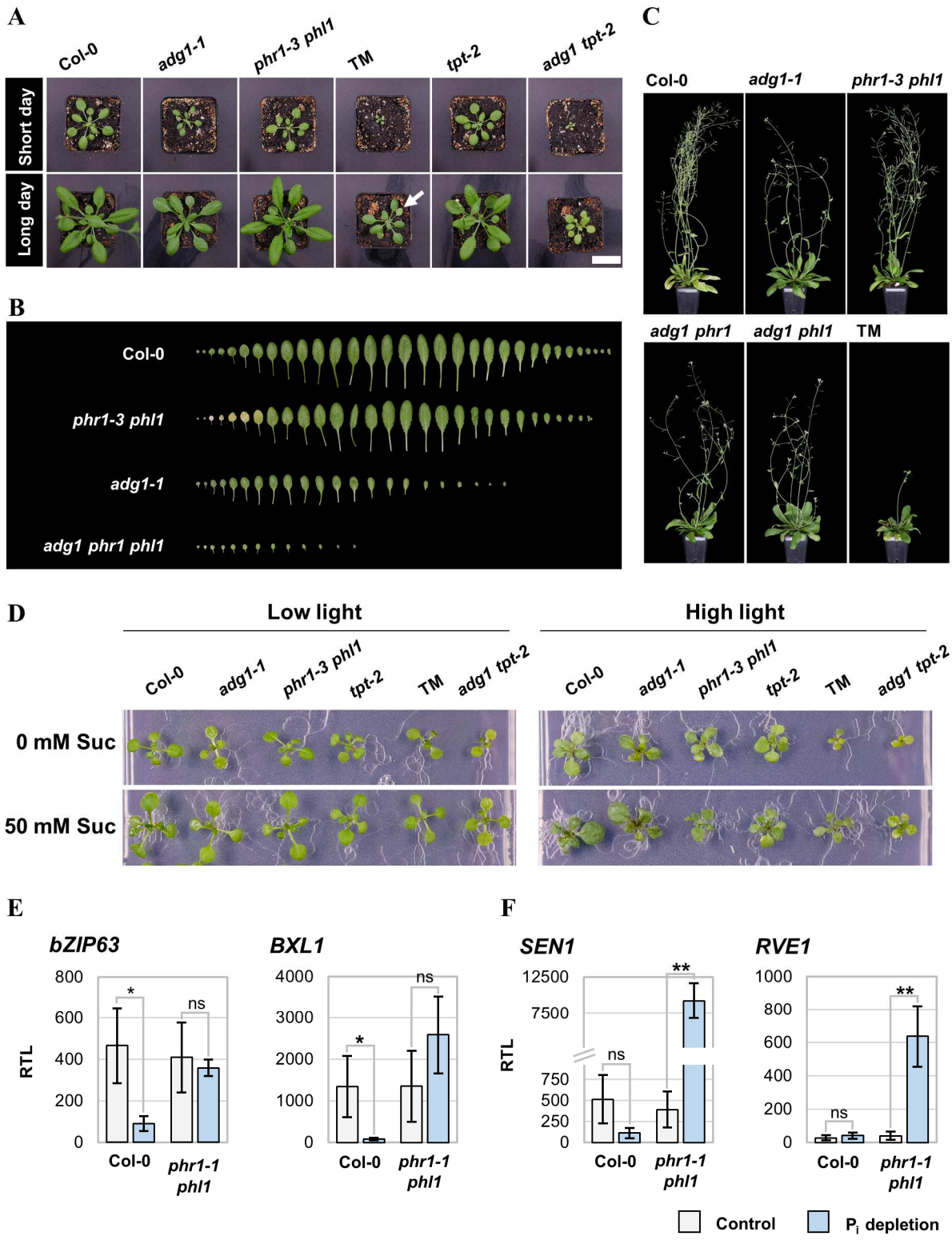

995

996 **Figure 5** Carbohydrate metabolism is affected by *phr1 phl1* mutation. **A-D,** Phenotypes of the
997 *adg1 phr1 phl1* triple mutant (**TM**). **A-C**, Plants were grown at 23°C and a light intensity of
998 100±10 µmol m^{-2} s^{-1}. **A,** Rosette habitus of plants grown under short-day (8 hours light period)
999 and long-day (16 h light period) conditions. Pictures were taken of representative plants after
1000 27 (short day) and 25 (long day) days of growth. The arrow indicates a senescent leaf. Bar,

2.5 cm. **B,** Leaves of 42 day-old plants grown under an 8-hours light regime were aligned according to age (starting with the cotyledons on the left hand side). **C,** Inflorescences of wildtype (Col-0), *adg1-1*, *phr1-3 phl1*, and derived genotypes showing delay of the transition to flowering in the TM. Pictures were taken of representative plants after 42 days of growth under a 16-hours light regiment. **B, C,** Backgrounds were manually removed for better visualization. **D**, High-light sensitivity of TM and growth promotion by exogenous sucrose. Seedlings were grown in long-day conditions under low light (50±5 µmol m^{-2} s^{-1}) or high light (320±30 µmol m^{-2} s^{-1}) on rich media with or without sucrose added. Media-containing square petri dishes were positioned horizontally. Pictures were taken after 14 days of growth. **E, F**, Carbohydrate responsive gene expression is affected under P_i starvation. qRT-PCR analysis of carbohydrate-responsive transcripts which are downregulated in shoots of the wildtype (E), or upregulated in shoots of *phr1-1 phl1* mutant seedlings (F) grown for 7 days on rich medium containing 0.5 % sucrose, and for additional 8 days on media with 0.5 % sucrose and either 2.5 mM (control, light grey bars), or 0 mM (P_i depletion, blue bars) KH_2PO_4 added. Transcript levels were calculated relative to the level of *PP2A* transcript as $1000 \cdot 2^{-\Delta CT}$. Bars represent means ± standard deviations; n = 3 independent experiments. One-way ANOVA with Tukey HSD follow-up test and Bonferroni alpha correction for contrasts; ** P <0.01, * P <0.05, ns, no significant difference.

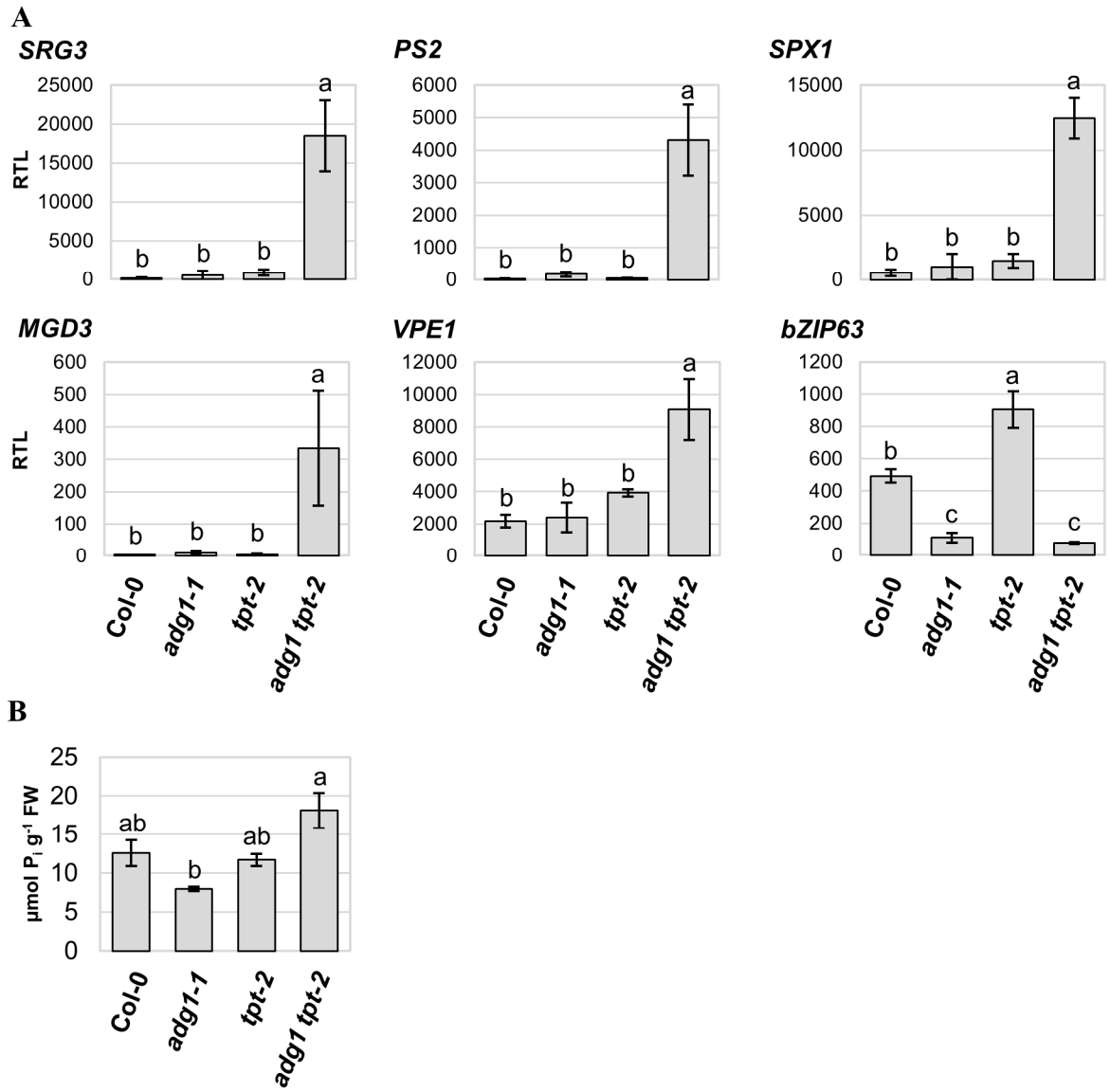

Figure 6 Constitutive P_i starvation transcription in rosette leaves of *adg1 tpt-2*. **A, B,** Plants were grown on soil at a photon flux density of 90±10 µmol m^{-2} s^{-1} and sampled 135 min after onset of the 8-hours photoperiod after 5 weeks of growth. **A,** qRT-PCR analysis of the transcript levels of P_i starvation marker genes in rosette leaves of wildtype (Col-0), *adg1-1*, *tpt-2*, and *adg1 tpt-2*. Transcript levels are $1000 \cdot 2^{-\Delta CT}$ relative to *PP2A*. Bars show means ± standard deviations. $n = 3$ independent experiments. One-way ANOVA with Tukey HSD follow-up test and Bonferroni alpha correction for contrasts; $P < 0.01$. **B,** P_i contents of rosette leaves. Means ± standard deviations are depicted. $n = 3$ independent experiments. Kruskal-Wallis test with DUNN's follow-up test and DUNN/Sidak alpha correction for contrasts; $P < 0.01$.

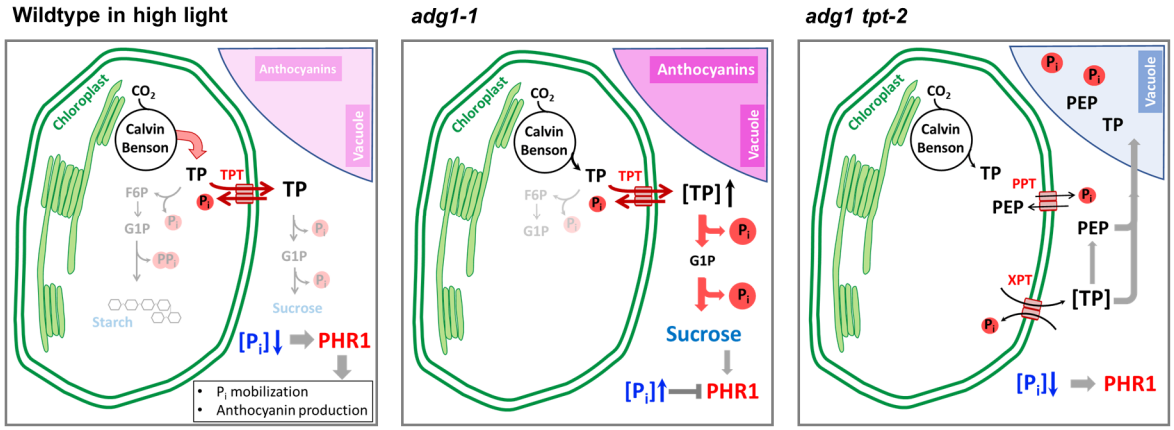

Figure 7 Model for PHR1 activation during imbalances in triose phosphate production and consumption. In wildtype mesophyll cells subjected to an increase in light intensity (left panel), triose phosphate (TP) production by the Calvin-Benson-Bassham cycle transiently exceeds the rates of TP utilization by starch and sucrose biosynthesis causing sequestration of free P_i. Increased export of TPs to the cytosol via the TPT leads to a decrease in P_i concentration in the cytosol which results in PHR1 activation. High PHR1 activity facilitates the mobilization of P_i from internal sources including the stimulation of starch accumulation, and, together with a signal derived from TPs or 3-phosphoglycerate (3-PGA) accumulation, PHR1 triggers anthocyanin production. In the *adg1-1* knockout (middle panel), TPs accumulate in the cytosol due to the lack of starch biosynthesis. High TP/3-PGA levels in the cytosol promote anthocyanin production and sucrose biosynthesis. High sucrose levels enhance P_i-starvation responses (Lei et al., 2011), while TP turnover confined to the cytosol keeps PHR1 activation at a moderate level. In *adg1 tpt-2* (right hand side panel), TP export relies on the xylulose 5-phosphate/P_i translocator (XPT) (Hilgers et al., 2018), keeping sucrose biosynthesis at low levels (Schmitz et al., 2012). TPs are partially consumed by glycolysis and imported back into the chloroplast by the phosphoenolpyruvate (PEP)/P_i translocator (PPT). Another portion of TPs and PEP is transferred to the vacuole where P_i is released by phosphatase activity. However, overall release of free P_i in the cytosol is low thus keeping PHR1 activity at high levels.